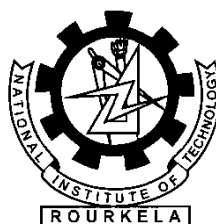


# **STUDY ON BOUNDARY SHEAR STRESS DISTRIBUTION IN MEANDERING TRAPEZOIDAL OPEN CHANNEL FLOW**

A THESIS SUBMITTED IN PARTIAL FULFILLMENT  
OF THE REQUIREMENTS FOR THE DEGREE OF

**Bachelor of Technology  
In  
CIVIL ENGINEERING**

By  
**PRITAM SAHANA (10401005)  
MRUTYUNJAYA SAHU (10501033)**



**Department of Civil Engineering  
National Institute of Technology  
Rourkela-769008  
May 2009**



**Department of Civil Engineering**

**National Institute of Technology**

**Rourkela-769 008**

**May 2009**

### **CERTIFICATE**

This is to certify that thesis entitled, “Study On Boundary Shear Stress Distribution in Meandering Trapezoidal Open Channel Flow” submitted by Pritam Sahana in partial fulfillment of the requirements for the award of Bachelor of Technology Degree in Mechanical Engineering at National Institute of Technology, Rourkela (Deemed University) is an authentic work carried out by him under my supervision and guidance.

To the best of my knowledge, the matter embodied in this thesis has not been submitted to any other university/ institute for award of any Degree or Diploma.

Dr. K. C. Patra

Professor

Dept. of Civil Engineering

National Institute of Technology

Rourkela-769008

## **Acknowledgements**

I wish to specially acknowledge the guidance given to me by Dr. K. C. Patra & Dr. K. K. Khatua in this present work without which it would not have been possible. I am also grateful to the Civil Engineering Department for allowing me to utilize all the facilities required for my work. I wish to acknowledge the Laboratory Assistant Mr. Pitambar Rout for his invaluable help.

PRITAM SAHANA  
DEPARTMENT OF CIVIL ENGINEERING  
NATIONAL INSTITUTE OF TECHNOLOGY, ROURKELA

## **ABSTRACT**

The determination of boundary shear stress distribution in meandering trapezoidal open channel flows is crucial in many critical engineering problems such as channel design, calculation of energy losses and sedimentation and in the study of shear stress distribution. In this study, velocity distribution is experimentally investigated in a smooth rectangular open channel. Wall shear stresses are calculated using measured local velocities. Assuming logarithmic velocity distribution along perpendiculars to a wetted perimeter, wall shear stresses were calculated. With the purpose of obtaining shear stress distributions at the walls and at the bed of an open channel, experimental data available in literature, for smooth open channels and smooth trapezoidal ducts, are analyzed and confronted.

**Keywords:** Shear stress distribution, shear stresses, aspect ratio, trapezoidal channels.



## **Contents**

- 1. Introduction**
  - 1.1 Open Channel Hydraulics
  - 1.2 Geometric Properties Necessary for Analysis
  - 1.3 Types of flow
  - 1.4 Review of the literature
- 2. Experimental Procedure and Analysis**
  - 2.1 Experimental Setup
  - 2.2 Measurement of Shear Stress
  - 2.3 Velocity Distribution in an Open channel flow
  - 2.4 Experimental Data
  - 2.5 Velocity Contour
  - 2.6 Theoretical Analysis
- 3. Boundary Shear Stress Distribution**
- 4. Numerical Evaluation of Boundary stress distribution in meandering Channel**
- 5. Results**
- 6. Validation of results**
- 7. Conclusion**
- 8. Reference**
- 9. Photo Gallery**

# INTRODUCTION

## 1.1 OPEN CHANNEL HYDRAULICS

Open channels may be of polished metal to natural channels with long grass and roughness that may also depend on depth of flow. Open channel flows are found in large and small scale. For example the flow depth can vary between a few cm in water treatment plants and over 10m in large rivers. The mean velocity of flow may range from less than 0.01 m/s in tranquil waters to above 50 m/s in high head spillways. The range of total discharges may extend from 0.001 l/s in chemical plants to greater than 10000 m<sup>3</sup>/s in large rivers or spillways. Open channel flow is driven by gravity rather than by pressure work as in pipes. Artificial channels are channels made by man. They include irrigation canals, navigation canals, spillways, sewers, culverts and drainage ditches. They are usually constructed in a regular cross-section shape throughout – and are thus prismatic channels (they don't widen or get narrower along the channel. In the field they are commonly constructed of concrete, steel or earth and have the surface roughness' reasonably well defined (although this may change with age particularly grass lined channels.) Analysis of flow in such well defined channels will give reasonably accurate results.

## 1.2 Geometric properties necessary for analysis

For analysis various geometric properties of channel cross-section are required. The commonly needed geometric properties are shown in the figure below and defined as:

Depth ( $y$ ) – the vertical distance from the lowest point of the channel section to the free surface.

Area ( $A$ ) – the cross-sectional area of flow, normal to the direction of flow.

Wetted perimeter ( $P$ ) – the length of the wetted surface measured normal to the direction of flow.

Hydraulic radius ( $R$ ) – the ratio of area to wetted perimeter ( $A/P$ )

Hydraulic mean depth ( $D_m$ ) – the ratio of area to surface width ( $A/B$ )

Aspect Ratio – the ratio of surface width and depth

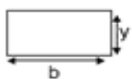
	Rectangle
	
Area, $A$	$by$
Wetted perimeter $P$	$b + 2y$
Top width $B$	$b$
Hydraulic radius $R$	$by / (b + 2y)$
Hydraulic mean depth $D_m$	$y$

Table of equation for rectangular and trapezoidal channel

## **1.3 TYPES OF FLOW**

### **Steady and Unsteady Flow**

Flow in a channel is said to be steady if the flow characteristics at any point does not change with time. However, in case of prismatic channels the conditions of steady flow maybe obtained if only the depth of flow does not change with time. On the other hand, if any of the flow characteristics changes with time the flow is unsteady. Most of the open channel problems involve the study of flow under steady conditions. In our experimental investigation, the flow is steady.

### **Uniform and Non-Uniform Flow**

Flow in a channel is said to be uniform if the depth, slope, cross-section and velocity remain constant over a given length of the channel. Obviously a uniform flow can occur only in a prismatic channel in which the flow will be uniform if only the depth of flow is same at every section of the channel. Flow in channels is termed as non uniform if the depth of flow changes from section to section. In our experimental investigation the flow is uniform.

### **Laminar flow and turbulent flow**

The flow in channels is also characterised by as laminar, turbulent or in a transitional state, depending on the relative effect of viscous and inertia forces and Reynolds number (Re) is a measure of this effect. However, the Reynolds no. flow in channels is commonly defined as,

$$Re = \rho VR / \mu$$

Where, V is the mean velocity of flow,

R is the hydraulic radius of the channel section

and  $\mu, \rho$  are respectively absolute viscosity of water and mass density.

On the basis of experimental data it has been found that up to Re equal to 500 to 600, the flow in channels maybe considered to be laminar and for Re greater than 2000, the flow in channels is turbulent.

### **Froude Number**

Gravity is a predominant force in the case of channel flow. As such, depending on the relative effect of gravity and inertia forces the channel flow maybe designated as sub-critical, critical or super critical. The ratio of the inertia and the gravity forces is another dimensionless parameter called Froude number (Fr), which is defined as

$$Fr = V / (gD)^{0.5}$$

Where V is the mean velocity of flow

g is acceleration due to gravity

D is hydraulic depth of channel section which is equal to (A/T)

A is the wetted area

T is the top width of the channel section at the free surface

When  $Fr$  equal to 1, the channel flow is said to be in a critical state, if  $Fr$  less than 1 then flow is described as sub-critical or streaming, if the  $Fr$  is greater than 1 the flow is said to be supercritical or rapid.

## FLOW OF COMPOUND CHANNEL

When the flow in natural or man made channel sections exceed the main channel depth, the water comes into the adjoining floodplains and carries part of the river discharge.

Due to different hydraulic conditions prevailing in the river and floodplain, the mean velocity in the main channel and in the floodplain are different.

It naturally generates a dragging or retarding force on the flow through the main channel and the main channel exerts a pulling or accelerating force on the flow over floodplains.

The relative “pull” and “drag” of the flow between faster and slower moving sections of a compound section complicates the momentum transfer between them.

Failure to understand this process leads to either overestimate or underestimate the discharge leading to the faulty design of a channel section. This causes frequent flooding at its lower reaches.

Meandering and the flow interaction between main channel and its adjoining flood plains are those natural processes that have not been fully understood.

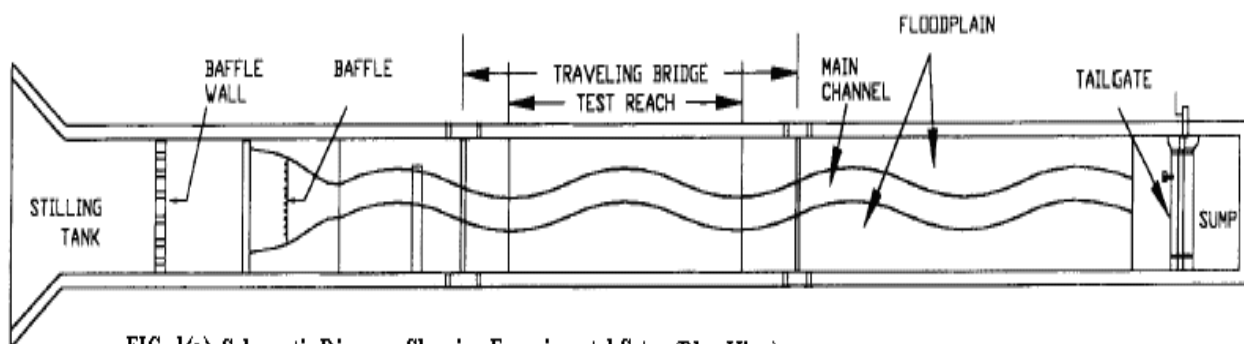
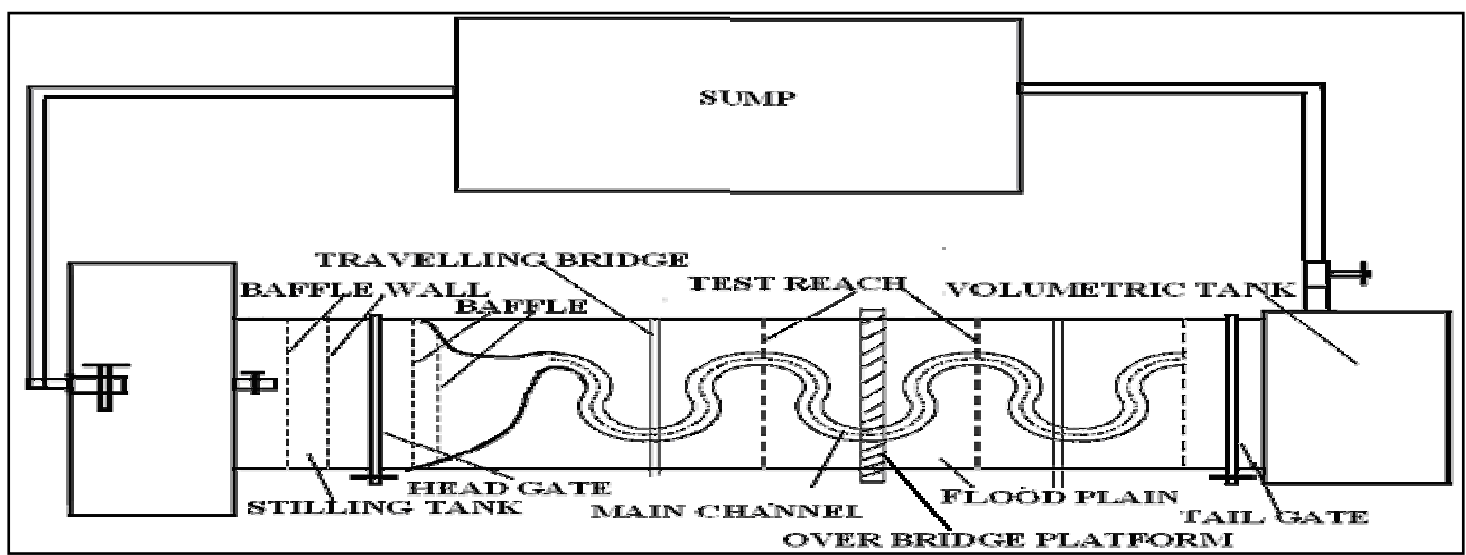
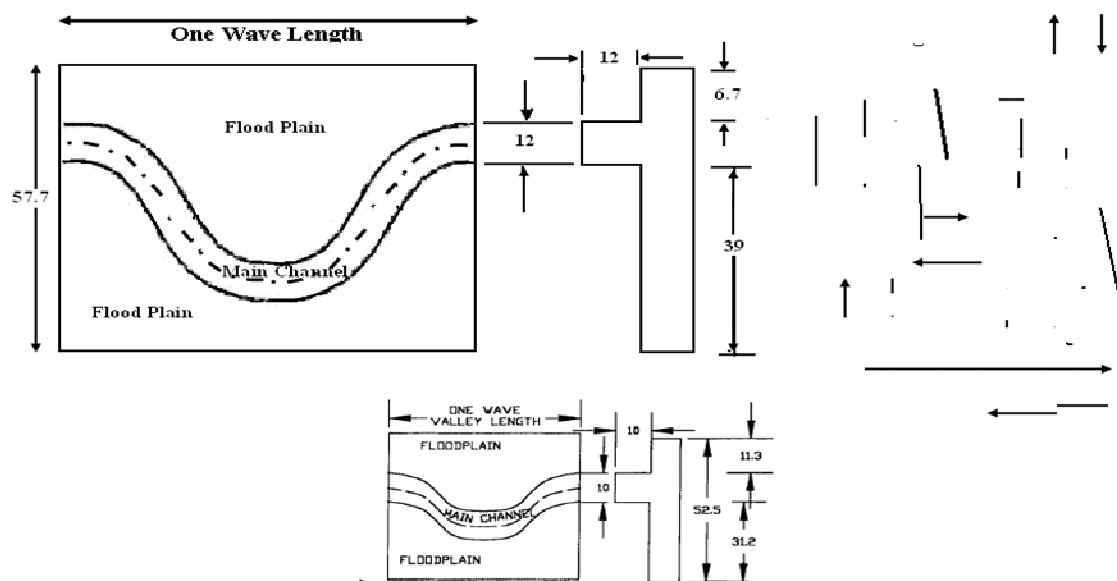
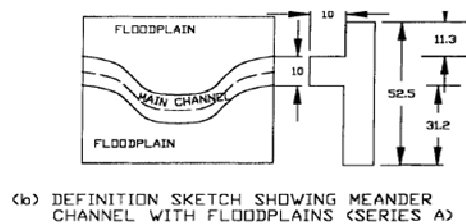


FIG. 1(a) Schematic Diagram Showing Experimental Setup (Plan View)

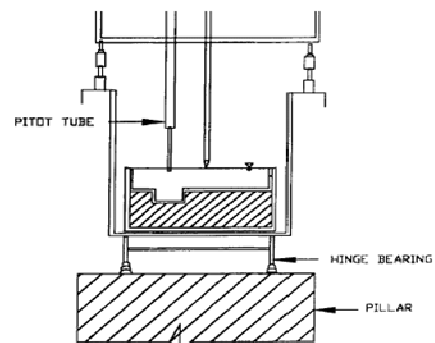




(b) DEFINITION SKETCH SHOWING MEANDER CHANNEL WITH FLOODPLAINS (SERIES A)

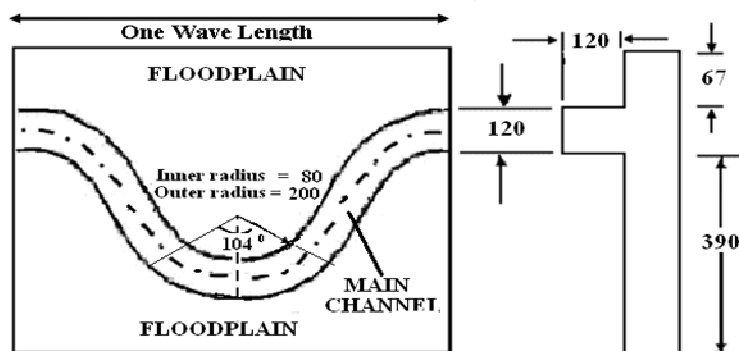
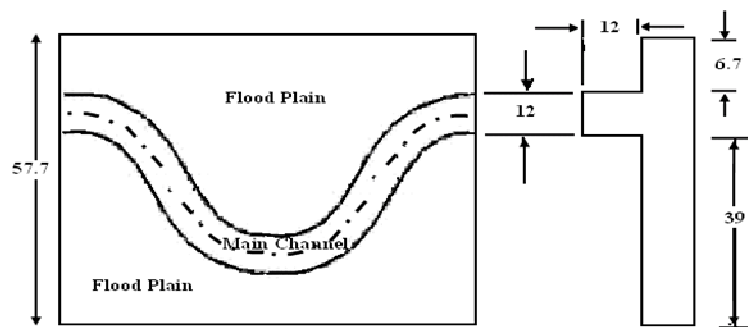


(b) DEFINITION SKETCH SHOWING MEANDER CHANNEL WITH FLOODPLAINS (SERIES A)

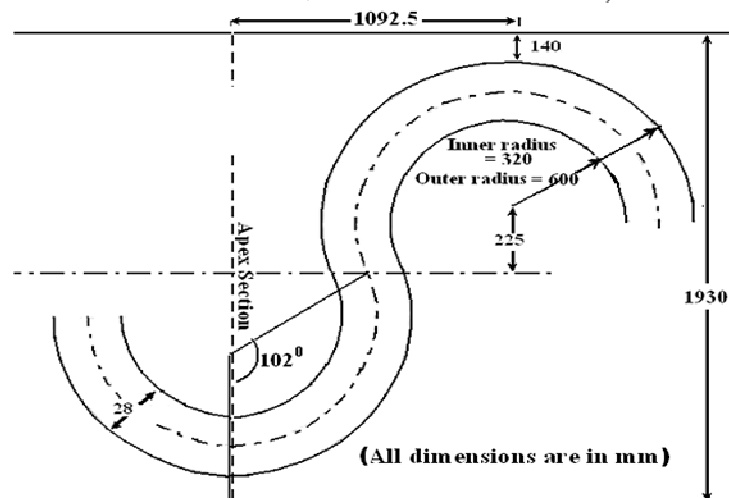


(c) CHANNEL SECTION

FIG. 2. Schematic Diagram Showing Experimental Setup



(All dimensions are in mm)



(All dimensions are in mm)

104°

102°

102°

## **1.4REVIEW OF LITERATURE**

### **SIMPLE MEANDER CHANNELS**

The Meandering channel flow is considerably more complex than constant curvature bend flow. The flow geometry in meander channel due to continuous stream wise variation of radius of curvature is in the state of either development or decay or both. The following important studies are reported concerning the flow in meandering channels.

Hook (1974) measured the bed elevation contours in a meandering laboratory flume with movable sand bed for various discharges. For each discharge he measured the bed shear stress, distribution of sediment in transport and the secondary flow and found that with increasing discharge, the secondary current increased in strength.

Chang (1984 a) analyzed the meander curvature and other geometric features of the channel using energy approach. It established the maximum curvature for which the river did the last work in turning, using the relations for flow continuity, sediment load, resistance to flow, bank stability and transverse circulation in channel bends. The analysis demonstrated how uniform utilization of energy and continuity of sediment load was maintained through meanders.

### **COMPOUND CHANNELS IN STRAIGHT REACHES**

While simple channel sections have been studied extensively, compound channels consisting of a deep main channel and one or more floodplains have received relatively little attention. Analysis of these channels is more complicated due to flow interaction taking place between the deep main channel and shallow floodplains. Laboratory channels provide the most effective alternative to investigate the flow processes in compound channels as it is difficult to obtain field data during over bank flow situations in natural channels. Therefore, most of the works reported are experimental in nature. Sellin (1964) confirmed the presence of the "kinematics effect" reported by Zheleznyakov(1965) after series of laboratory studies and presented photographic

evidence of the presence of a series of vortices at the interface of main channel and flood plain. He studied the channel velocities and discharge under both interacting and isolated conditions by introducing a thin impermeable film at the junction. Under isolated condition, velocity in the main channel was observed to be more and under interacting condition the velocity in floodplain was less.

Rajaratnam and Ahmadi (1979) studied the flow interaction between straight main channel and symmetrical floodplain with smooth boundaries. The results demonstrated the transport of longitudinal momentum from main channel to flood plain. Due to flow interaction, the bed shear in floodplain near the junction with main channel increased considerably and that in the main channel decreased. The effect of interaction reduced as the flow depth in the floodplain increased.

Knight and Demetriou (1983) conducted experiments in straight symmetrical compound channels to understand the discharge characteristics, boundary shear stress and boundary shear force distributions in the section. They presented equations for calculating the percentage of shear force carried by floodplain and also the proportions of total flow in various sub-areas of compound section in terms of two dimensionless channel parameters. For vertical interface between main channel and floodplain the apparent shear force was found to be more for low depths of flow and for high floodplain widths. On account of interaction of flow between floodplain and main channel it was found that the division of flow between the subsections of the compound channel did not follow a simple linear proportion to their respective areas.

Knight and Hamed (1984) extended the work of Knight and Demetriou (1983) to rough floodplains. The floodplains were roughened progressively in six steps to study the influence of different roughness between floodplain and main channel to the process of lateral momentum transfer. Using four dimensionless channel parameters, they presented equations for the shear force percentages carried by floodplains and the apparent shear force in vertical, horizontal diagonal and bisector interface plains. The apparent shear force results and discharge data provided the weakness of these four commonly adopted design methods used to predict the discharge capacity of the compound channel.



## **MEANDERING COMPOUND CHANNELS**

There are limited reports concerning the characteristics of flow in meandering compound sections.

A study by United States water ways experimental station (1956) related the channel and floodplain conveyance to geometry and flow depth, concerning, in particular, the significance of the ratios of channel width to floodplain width and meander belt width to floodplain width in the meandering two stage channel.

Toebe and Sooky (1967) were probably the first to investigate under laboratory conditions the hydraulics of meandering rivers with floodplains. They attempted to relate the energy loss of the observed internal flow structure associated with interaction between channel and floodplain flows. The significance of helicoidal channel flow and shear at the horizontal interface between main channel and floodplain flows were investigated. The energy loss per unit length for meandering channel was up to 2.5 times as large as those for a uniform channel of same width and for the same hydraulic radius and discharge. It was also found that energy loss in the compound meandering channel was more than the sum of simple meandering channel and uniform channel carrying the same total discharge and same wetted perimeter. The interaction loss increased with decreasing mean velocities and exhibited a maximum when the depth of flow over the floodplain was less. For the purpose of analysis, a horizontal fluid boundary located at the level of main channel bank full stage was proposed as the best alternative to divide the compound channel into hydraulic homogeneous sections. Helicoidal currents in meander floodplain geometry were observed to be different and more pronounced than those occurring in a meander channel carrying in bank flow. Reynold's number ( $R$ ) and Froude number ( $F$ ) had significant influence on the meandering channel flow. Ghosh and Kar (1975) reported the evaluation of interaction effect and the distribution of boundary shear stress in meander channel with floodplain. Using the relationship proposed by Toebe and Sooky (1967) they evaluated the interaction effect by a parameter ( $W$ ). The interaction loss increased up to a certain floodplain depth and there after it decreased. They concluded that channel geometry and roughness distribution did not have any influence on the interaction loss.

Ervine, Willetts, Sellin and Lorena (1993) reported the influence of parameters like sinuosity, boundary roughness, main channel aspect ratio, and width of meander belt, flow depth above bank full level and cross sectional shape of main channel affecting the conveyance in the meandering channel. They quantified the effect of each parameter through a non-dimensional discharge coefficient  $F^*$  and reported the possible scale effects in modeling such flows.

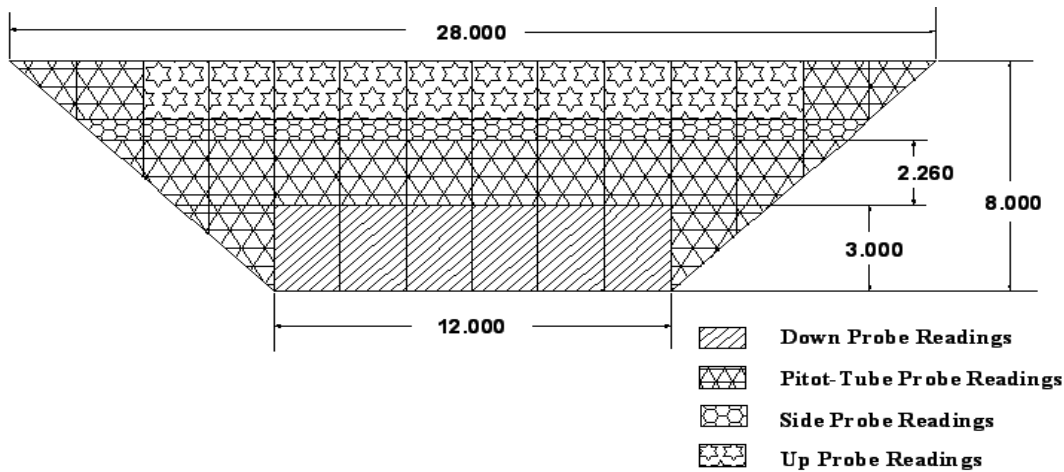
Patra and Kar (2000) reported the test results concerning the boundary shear stress, shear force, and discharge characteristics of compound meandering river sections composed of a rectangular main channel and one or two floodplains disposed off to its sides. They used five dimensionless channel parameters to form equations representing the total shear force percentage carried by floodplains. A set of smooth and rough sections is studied with an aspect ratio varying from 2 to 5. Apparent shear forces on the assumed vertical, diagonal, and horizontal interface plains are found to be different from zero at low depths of flow and change sign with an increase in depth over the floodplain. A variable-inclined interface is proposed for which apparent shear force is calculated as zero. Equations are presented giving proportion of discharge carried by the main channel and floodplain. The equations agreed well with experimental and river discharge data.

Patra and Kar (2004) reported the test results concerning the velocity distribution of compound meandering river sections composed of a rectangular main channel and one or two floodplains disposed off to its sides. They used dimensionless channel parameters to form equations representing the percentage of flow carried by floodplains and main channel sub sections.

Shiono, Romainh & Knight (2004) carried out discharge measurements for over bank flow in a two-stage meandering channel with various bed slopes, sinuosities, and water depths. The effect of bed slope and sinuosity on discharge was found to be significant. A simple design equation for the conveyance capacity based on dimensional analysis is proposed. This equation may be used to estimate the stage-discharge curve in a meandering channel with over bank flow.

## **2.1 EXPERIMENTAL WORK**

The work presented in this paper is based on series of highly meandering channels having distinctly different sinuosity and geometry. Experiments are carried out to examine the effect of secondary currents, channel sinuosity, and cross section geometry on the value of boundary shear. First the 3-dimensional velocities at a number of pre defined grid points across the channel section are measured using 16-Mhz Micro ADV (Acoustic Doppler Velocity-meter). Using these velocity data close to the surface, the boundary shear at various points on the channel boundaries are evaluated from semi log plot of velocity distribution as well as by using numerical finite difference solution.



## **EXPERIMENTAL PROCEDURE**

### **Determination of Channel Slope**

By blocking the tail end, the impounded water in the channel is allowed to remain standstill. The levels of channel bed and water surface are recorded at a distance of one wavelength along its centerline. The mean slope for each type of channel is obtained by dividing the level difference between these two points by the length of meander wave along the centerline. The valley slope for meandering compound channels are kept same and is equal to 0.0054.

### **Measurement of Discharge and water surface elevation**

A point gauge with a least count of 0.01cm was used to measure the water surface elevation above the bed of main channel or flood plain. As mentioned before, a measuring tank located at the end of test channel receives water flowing through the channels. Depending on the flow rate the time of collection of water in the measuring tank varies between 50 to 240 seconds, lower one for higher discharge. The change in the mean water level in the tank for the time interval is recorded. From the knowledge of the volume of water collected in the measuring tank and the corresponding time of collection, the discharge flowing in the experimental channel is obtained.

### **Measurement of Velocity and its Direction**

16-MHz Micro ADV (Acoustic Doppler Velocity meter) from the original Son-Tek, San Diego, Canada, is the most significant breakthrough in 3-axis (3D) Velocity meter technology. The higher acoustical frequency of 16 MHz makes the Micro-ADV the optimal instrument for laboratory study. After setup of the Micro ADV with the software package it is used for taking high-quality three dimensional Velocity data at different points of the flow area are received to the ADV-processor. Computer shows the raw data after compiling the software package of the processor. At every point the instrument is recording a number of velocity data for a minute. With the statistical analysis using the installed software, the mean value of the point velocities (three dimensional) were recorded for each flow depths. The Micro -ADV uses the Doppler shift principle to measure the velocity of small particles, assuming to be moving at velocities similar to the fluid. Velocity is resolved into three orthogonal components (Tangential, radial and vertical), and measured in a volume 5 cm below the sensor head, minimizing interference of the flow field, and allowing measurements to be made close to the bed.

The Micro ADV has the Features like

- Three-axis velocity measurement
- High sampling rates -- up to 50 Hz
- Small sampling volume -- less than 0.1 cm<sup>3</sup>
- Small optimal scatterer -- excellent for low flows
- High accuracy: 1% of measured range
- Large velocity range: 1 mm/s to 2.5 m/s

- Excellent low-flow performance
- No recalibration needed
- Comprehensive software

As the ADV is unable to read the upper layer velocity i.e. up to 5cm from free surface so A standard Prandtl type micro-pittot tube in conjunction with a water manometer of accuracy of 0.012 cm is also used for the measurement of point velocity readings at some specified location for the upper 5cm region from free surface across the channel.

### **The Acoustic-Doppler Velocimeter (ADV)**

#### **Working principle**

The Acoustic Doppler Velocimeter (ADV) was used to measure the 3-Dimensional velocity components. It is a remote sensing 3-D velocity sensor which transmits acoustic pulses into water. These pulses are then scattered by the particles present in water. The echo is received by the receivers of the ADV and the Doppler shift is calculated from the segments of the echo. The echo is Doppler shifted in proportion to the particle velocity. The naming convention, types and working principle of the ADV are shown in Fig. 2. There are four types of ADV probes: (i) 3-D down-looking probe (ii) 3-D up-looking probe (iii) 3-D side looking probe and (iv) 2- D side-looking probe. Among these four types of probes, two types namely 3-D down-looking probe and 3-D side-looking probe were employed for this study. In the present study the x-axis of the side-looking probe indicates the down flow, downward direction being positive; the y-axis indicates the transverse flow and the z-axis indicates the flow along the line of orientation with direction away from the pier being positive.

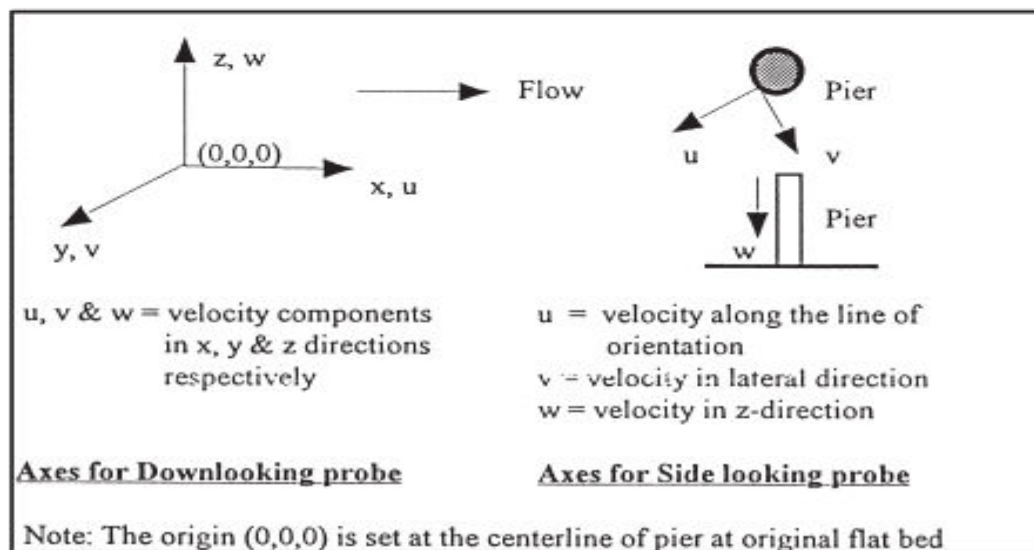
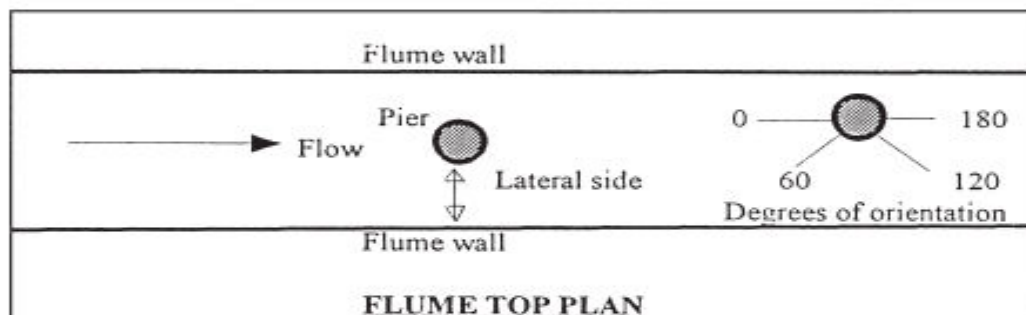
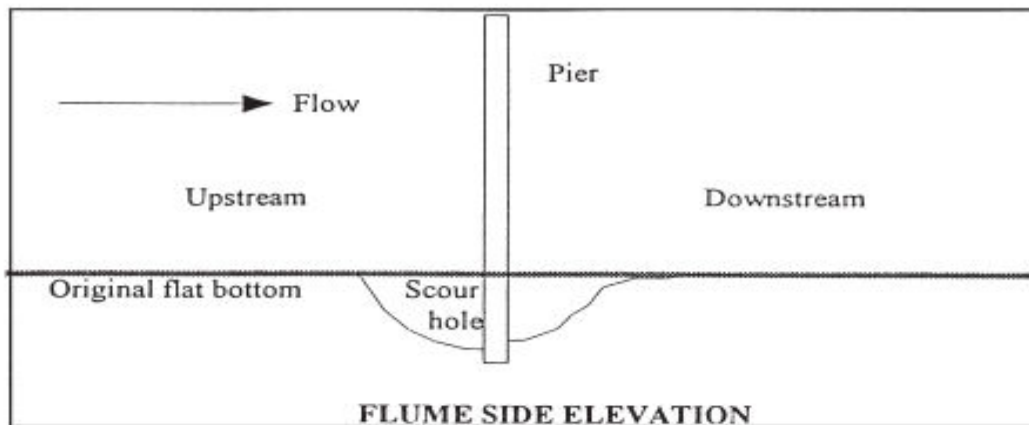


Fig. 1. Pier model and the axes for the ADV probes.

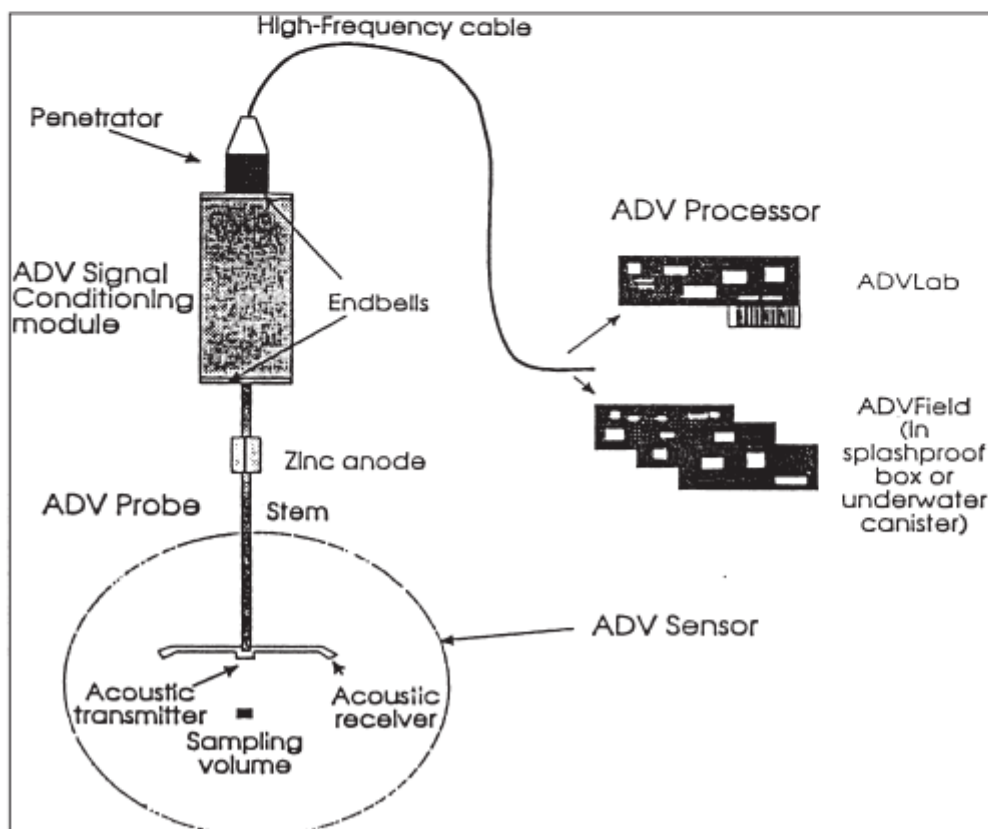
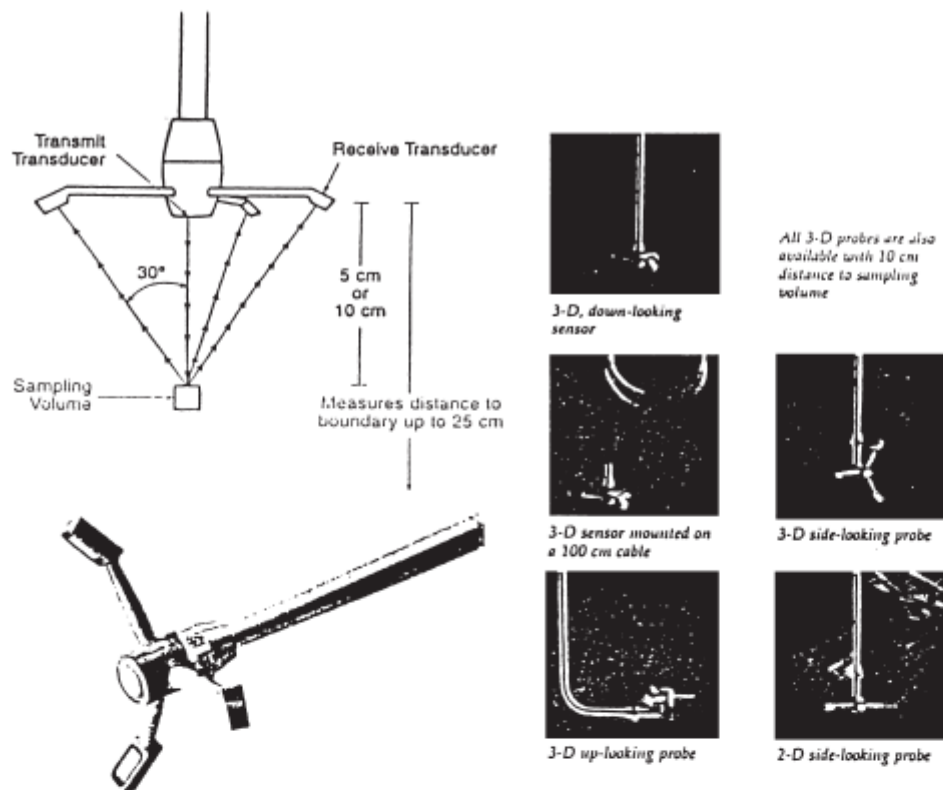


Fig. 2. The ADV - Naming convention, types and working principle.

## **2.2 VELOCITY DISTRIBUTION IN OPEN CHANNEL FLOW**

The velocity of flow at any channel section is not uniformly distributed. The non uniform distribution of velocity in an open channel is due to the presence of a free surface and a frictional resistance along the channel boundary. The velocity distribution in a channel is measured either with the help of a Pitot tube or a current meter. The velocity distribution in an open channel flow depends on various factors such as the shape of the section, the roughness of the channel and the presence of bends in the channel alignment. In a straight reach of a channel maximum velocity usually occurs below the free surface at a distance of 0.05 to 0.15 of the depth of flow. The mean velocity of flow in a channel section can be computed from the vertical velocity distribution curve obtained by actual measurements. It is observed that the velocity at 0.6 depth from the free surface is very close to the mean velocity of flow in vertical section. A still better approximation for the mean velocity of flow is obtained by taking the average of the velocities measured at 0.2 depths and 0.8 depths from the free surface.

## **2.3 CALCULATION OF SHEAR STRESS**

In open channels, it is often necessary to find the bed shear stress to calculate the velocities and flow rate, possible erosion of the bed as well as the rate of sediment transport. A simple method is to use the Preston tube (Preston 1954), in which the dynamic pressure  $\Delta p$  measured by a total head tube located on the boundary facing the flow, is correlated with the boundary shear stress using the law of the wall. For smooth boundaries, the calibration curve provided by Patel(1965) is generally used whereas for uniformly rough boundaries, the calibration curves developed by Hollingshead and Rajaratnam(1980) may be used.

In our study the principal instrument used in the study was an Pitot tube. The probe was used to measure the local velocity at different depths. The fundamental premise of the work is that velocity profiles can be used to determine, through statistical analysis, the characteristic velocity scale of the local flow,  $U^*$ , the local roughness parameter,  $Z_0$ , and the local displacement of the origin,  $D$ . Well known logarithmic relation gives the equation as-

$$\frac{u}{U^*} = \frac{1}{\kappa} \ln \left( \frac{z}{Z_0} \right)$$

where  $z$  = vertical position above the bed, including  $D$ ; and  $\kappa$  is von Karman's constant (taken to be constant). Using Prandtl-von Karman universal velocity distribution law,  $[(v/V^*) = 2.5 \log_{10}(h/h')]$ ,

Keulegan has derived the following equation for the velocity in channels.

For smooth channels

$$(v/V^*) = 5.75 \log_{10}(h/h') \quad \dots\dots\dots(1)$$

Where  $v$  is the mean velocity of flow,

$V^*$  is the shear velocity,



h is the depth of flow,  
h' is the finite distance above the boundary where the velocity is equal to zero.

Now for two different depth of flow ( h<sub>1</sub> and h<sub>2</sub>) , eqn 1 can be rewritten as

$$(v_1/V^*) = 5.75 \log_{10}(h_1/h') \dots\dots\dots(2)$$

$$(v_2/V^*) = 5.75 \log_{10}(h_2/h') \dots\dots\dots(3)$$

Subtracting (3) from (2), we get

$$(v_1 - v_2)/V^* = 5.75 \log_{10} (h_1/h_2),$$

$$\text{or, } V^* = (v_1 - v_2) / 5.75 \log_{10} (h_1/h_2).$$

For steady uniform flow in an open channel, gravity forces causing the flow must be equal to boundary shear forces. The channel depth is approximately equal to the hydraulic radius R<sub>h</sub> for a very wide-open channel. R<sub>h</sub> is equal to the ratio of the cross-section area A to the wetted perimeter P. Therefore, the shear stress at the channel bed is expressed as

$$T_0 = wR_h S_0$$

Where S<sub>0</sub> is the slope of the channel bed,

w is the unit weight of water.

Now,

$$V^* = (T_0/\rho)^{1/2}$$

$$\text{So, } T_0 = \rho [ (v_1 - v_2) / 5.75 \log_{10} (h_1/h_2) ]^2 \dots\dots\dots(4)$$

This equation is used in calculating the local shear stress in the open channel section.

## 2.4 EXPERIMENTAL DATA

Depth of water = 6cm

Discharge = area\*ht of water rise in tank/time taken

Area of collecting tank = 83190 cm<sup>2</sup>

Point	Depth of water	Coordinate	Vx	Vy	Vz
DL 1	0.43	1	40.758	-2.5	1.168
	0.53	2	40.388	0.526	0.350
	0.66	3	10.938	-1.286	1.762
	0.76	4	39.294	3.378	0.620
	0.86	5	36.070	1.998	0.354
	0.93	6	35.594	0.704	1.124
	1.10	7	34.855	-0.248	0.540
	1.53	8	35.874	-1.112	0.554
UL 1	0.68	1	30.326	1.780	0.380
	0.80	2	37.912	5.640	-5.714
	0.81	3	39.670	3.668	-0.896
DL 2	0.49	1	39.938	3.392	-0.128
	0.66	2	32.667	1.385	-1.035
	0.70	3	38.610	3.812	0.135
	0.82	4	36.932	2.362	0.604
	0.95	5	39.156	1.546	0.876
	1.32	6	34.327	0.717	0.375
UL 2	0.68	1	38.782	8.076	-2.848
	0.80	2	31.544	6.922	-1.962
DL 3	0.44	1	37.268	-0.142	-0.730
	0.52	2	36.380	1.768	0.416
	0.62	3	38.900	6.384	-0.360
	0.76	4	33.432	10.910	0.274
	0.86	5	36.472	5.156	-0.048
	0.97	6	38.368	6.688	-0.533
UL 3	0.58	1	36.266	8.610	-2.466
	0.68	2	35.096	9.390	-2.482
DL 4	0.43	1	35.578	4.942	0.868
	0.55	2	37.700	1.504	0.174
	0.69	3	36.068	-3.132	0.482
	0.73	4	39.128	-1.998	0.692
	0.87	5	35.918	3.182	0.094

	0.95	6	36.618	1.624	-0.370
	1.33	7	35.888	-2.620	0.198
UL 4	0.64	1	33.566	10.103	-1.385
	0.66	2	37.027	6.938	-2.234

Depth of water = 6.4cm

Discharge = area\*ht of water rise in tank/time taken

Area of collecting tank = 83190 cm<sup>2</sup>

Point	Depth of water	Coordinate	Vx	Vy	Vz
DL 1	0.58	1	39.210	7.664	-0.568
	0.68	2	35.566	-9.273	-0.079
	0.73	3	38.338	-1.142	1.020
	0.80	4	39.510	0.454	1.238
	0.95	5	41.090	0.684	0.816
	1.28	6	35.730	-0.410	0.978
UL 1	0.94	1	35.543	1.132	-0.812
	1.37	2	34.964	3.606	0.934
DL 2	0.58	1	38.304	1.049	1.084
	0.64	2	35.460	2.520	1.272
	0.79	3	39.375	5.485	1.383
	0.85	4	41.766	0.952	0.976
	0.92	5	41.370	6.784	0.302
	1.28	6	32.902	7.362	0.490
UL 2	0.84	1	42.764	7.868	11.154
	1.13	2	46.510	4.630	-0.264
DL 3	0.58	1	38.304	1.049	1.084
	0.64	2	35.460	2.520	1.272
	0.79	3	39.375	5.485	1.383
	0.85	4	31.766	0.952	0.976
	0.92	5	37.370	6.784	0.302
	1.28	6	42.902	7.362	0.490
UL 3	0.75	1	42.182	7.080	-0.876
	1.30	2	34.100	3.922	1.416
DL 4	0.58	1	36.546	6.104	1.764
	0.66	2	35.398	1.140	0.736
	0.74	3	35.312	1.336	-0.070
	0.86	4	37.432	9.0288	1.360
	0.90	5	35.516	6.068	0.924

	1.37	6	33.802	6.558	1.448
UL 4	0.68	1	41.898	7.128	1.280
	1.41	2	42.350	12.258	1.790
	2.16	3	26.978	8.176	1.938
SL A11	0.69	1	1.5888	25.062	-0.394
(outer)	0.70	2	1.904	26.036	0.056
	0.98	3	3.188	24.428	0.454
SL A12	0.52	1	1.767	-20.259	-0.307
(inner)	0.62	2	1.472	-31.203	-1.010
	0.96	3	2.649	-30.671	-0.046

Depth of water = 7.2cm

Discharge = area\*ht of water rise in tank/time taken

Area of collecting tank = 83190 cm<sup>2</sup>

Point	Depth of water	Coordinate	Vx	Vy	Vz
DL 1	0.59	1	41.404	2.757	0.565
	0.69	2	42.740	-0.572	1.450
	0.76	3	38.974	1.106	1.176
	0.83	4	43.708	2.326	0.214
	0.92	5	36.656	-0.978	0.882
	1.14	6	39.043	1.508	0.732
	2.01	7	42.100	-0.248	0.254
UL 1	0.64	1	35.244	11.680	-0.270
	1.44	2	35.944	12.772	0.426
	2.17	3	37.442	12.389	-0.420
DL 2	0.41	1	41.308	-0.222	0.960
	0.57	2	42.368	1.906	1.736
	0.65	3	41.776	-0.580	1.044
	0.78	4	38.410	1.620	0.300
	0.87	5	39.772	0.822	1.040
	0.94	6	41.568	1.122	0.948
	1.06	7	38.720	2.004	0.094
	2.11	8	40.948	-0.184	0.056

<b>UL 2</b>	<b>0.82</b>	<b>1</b>	<b>18.102</b>	<b>11.582</b>	<b>-0.690</b>
	<b>1.46</b>	<b>2</b>	<b>19.584</b>	<b>13.064</b>	<b>-1.334</b>
	<b>2.03</b>	<b>3</b>	<b>18.042</b>	<b>15.926</b>	<b>-2.094</b>
	<b>2.85</b>	<b>17</b>	<b>40.470</b>	<b>10.665</b>	<b>-0.340</b>
	<b>2.97</b>	<b>18</b>	<b>41.971</b>	<b>12.576</b>	<b>0.114</b>
<b>DL 3</b>	<b>0.49</b>	<b>1</b>	<b>43.178</b>	<b>1.533</b>	<b>0.325</b>
	<b>0.59</b>	<b>2</b>	<b>43.720</b>	<b>2.062</b>	<b>0.263</b>
	<b>0.63</b>	<b>3</b>	<b>37.995</b>	<b>3.337</b>	<b>1.113</b>
	<b>0.72</b>	<b>4</b>	<b>33.202</b>	<b>0.095</b>	<b>0.653</b>
	<b>0.83</b>	<b>5</b>	<b>36.406</b>	<b>1.220</b>	<b>0.532</b>
	<b>0.93</b>	<b>6</b>	<b>42.467</b>	<b>0.113</b>	<b>0.053</b>
	<b>1.01</b>	<b>7</b>	<b>33.058</b>	<b>1.298</b>	<b>0.012</b>
	<b>2.16</b>	<b>8</b>	<b>34.940</b>	<b>0.778</b>	<b>0.664</b>
<b>UL 3</b>	<b>0.75</b>	<b>1</b>	<b>28.364</b>	<b>14.020</b>	<b>-0.722</b>
	<b>1.33</b>	<b>2</b>	<b>39.180</b>	<b>15.312</b>	<b>-2.180</b>
	<b>2.12</b>	<b>3</b>	<b>20.404</b>	<b>18.656</b>	<b>-1.086</b>
<b>DL 4</b>	<b>0.49</b>	<b>1</b>	<b>32.027</b>	<b>2.123</b>	<b>0.728</b>
	<b>0.58</b>	<b>2</b>	<b>38.550</b>	<b>1.682</b>	<b>1.428</b>
	<b>0.65</b>	<b>3</b>	<b>34.850</b>	<b>1.852</b>	<b>1.170</b>
	<b>0.74</b>	<b>4</b>	<b>43.190</b>	<b>1.508</b>	<b>1.996</b>
	<b>0.87</b>	<b>5</b>	<b>36.604</b>	<b>2.040</b>	<b>0.712</b>
	<b>0.94</b>	<b>6</b>	<b>36.204</b>	<b>1.616</b>	<b>0.714</b>
	<b>1.16</b>	<b>7</b>	<b>42.706</b>	<b>1.122</b>	<b>0.620</b>
	<b>2.15</b>	<b>8</b>	<b>42.338</b>	<b>0.534</b>	<b>-0.122</b>
<b>UL 4</b>	<b>0.68</b>	<b>1</b>	<b>40.898</b>	<b>7.128</b>	<b>1.280</b>
	<b>1.41</b>	<b>2</b>	<b>32.350</b>	<b>12.258</b>	<b>1.790</b>
	<b>2.16</b>	<b>3</b>	<b>26.978</b>	<b>8.176</b>	<b>1.938</b>
<b>SL A11</b>	<b>0.46</b>	<b>1</b>	<b>4.568</b>	<b>37.778</b>	<b>1.472</b>
<b>(outer)</b>	<b>0.55</b>	<b>2</b>	<b>1.910</b>	<b>39.020</b>	<b>0.666</b>
	<b>0.62</b>	<b>3</b>	<b>4.970</b>	<b>38.134</b>	<b>1.356</b>
	<b>0.74</b>	<b>4</b>	<b>4.644</b>	<b>42.288</b>	<b>1.216</b>
	<b>0.82</b>	<b>5</b>	<b>7.930</b>	<b>38.012</b>	<b>2.258</b>
	<b>0.94</b>	<b>6</b>	<b>-1.678</b>	<b>42.646</b>	<b>-1.006</b>
	<b>1.04</b>	<b>7</b>	<b>3.042</b>	<b>41.406</b>	<b>-0.818</b>
	<b>2.10</b>	<b>8</b>	<b>1.980</b>	<b>34.026</b>	<b>-1.546</b>
<b>SL A12</b>	<b>0.41</b>	<b>1</b>	<b>-2.874</b>	<b>-39.102</b>	<b>7.032</b>
<b>(inner)</b>	<b>0.56</b>	<b>2</b>	<b>1.398</b>	<b>-33.930</b>	<b>-0.530</b>

	0.69	3	2.492	-41.518	0.194
	0.74	4	-0.480	-42.586	-0.892
	0.80	5	-3.996	-35.794	-0.176
	0.94	6	-4.612	-43.712	-0.776
	1.08	7	1.244	-33.330	-0.280

Depth of water = 7.9cm

Discharge = area\*ht of water rise in tank/time taken

Area of collecting tank = 83190 cm<sup>2</sup>

Point	Depth of water	Coordinate	Vx	Vy	Vz
DL A1	0.44	1	33.876	1.939	3.697
	0.52	2	31.816	1.225	2.229
	0.60	3	27.050	0.292	1.998
	0.72	4	35.121	1.112	1.699
	0.82	5	21.249	-0.201	3.146
	1.09	7	36.343	-0.472	2.432
	1.14	8	32.331	4.048	0.730
	2.81	9	20.070	-3.045	1.559
UP A1	1.92	1	38.797	7.760	-2.236
	2.18	2	41.139	13.758	-1.943
	2.22	3	38.106	1.665	-1.454
	2.53	4	39.922	7.611	1.125
	2.65	5	37.586	2.132	-1.085
	2.8	6	39.184	2.667	-2.548
DL A2	0.44	1	29.491	-2.766	3.876
	0.54	2	36.501	-0.424	4.590
	0.68	3	30.513	-1.008	3.899
	0.74	4	18.313	-0.225	2.349
	0.88	5	34.663	-4.945	5.245
	0.94	6	23.096	0.049	2.960
	1.09	7	25.391	-0.245	3.308
	1.22	8	33.516	-5.078	4.500
	2.98	9			
UP A2	0.66	1	36.190	13.978	-0.702
	0.74	2	31.882	7.267	0.024
	0.88	3	45.368	7.275	-5.109
	0.90	4	35.011	13.077	-0.770
	1.00	5	44.776	3.042	-5.523

	1.12	6	38.380	17.801	-0.496
	2.85	7	40.470	10.665	-0.340
	2.97	8	41.971	12.576	0.114
DL A3	0.49	1	28.695	0.463	0.808
	0.59	2	38.864	-2.522	2.708
	0.62	3	24.700	-1.369	0.404
	0.72	4	32.937	-1.656	4.576
	0.81	5	24.989	-2.059	3.683
	0.97	6	6.898	1.019	0.279
	1.06	7	19.282	1.280	2.351
	1.15	8	36.991	-0.225	4.212
	2.60	9	31.441	-0.877	-0.091
	3.00	10	22.260	-0.757	-0.123
UP A3	0.75	1	36.997	14.347	-0.087
	0.86	2	39.284	15.488	-2.433
	0.94	3	38.972	17.315	-2.186
	1.03	4	40.587	17.926	-1.517
	1.28	5	41.919	11.744	-0.435
	2.67	6	42.869	24.214	-2.095
	2.83	7	42.119	23.222	-1.470
DL A4	0.47	1	33.948	0.351	4.201
	0.53	2	26.214	-2.003	2.525
	0.63	3	37.979	-1.747	-0.002
	0.74	4	23.297	-1.567	1.901
	0.83	5	31.177	-1.438	0.701
	0.92	6	23.011	-3.907	1.217
	1.01	7	33.575	-0.223	0.581
	1.27	8	29.206	-4.484	0.056
	2.90	9	33.065	1.151	-0.068
	3.00	10	40.556	-0.279	-0.041
UP A4	0.66	1	38.745	12.381	-3.468
	0.79	2	40.967	16.257	-3.657
	0.84	3	42.576	18.232	-1.658
	0.98	4	45.306	13.271	-3.005
	1.04	5	43.687	15.662	-3.296
	1.31	6	45.927	10.821	-1.714
	2.85	7	44.546	18.584	-1.426
	2.90	8	43.428	18.918	-0.963

<b>DL A5</b>	<b>0.43</b>		<b>32.945</b>	<b>1.643</b>	<b>1.445</b>
	<b>0.55</b>	<b>1</b>	<b>34.069</b>	<b>0.810</b>	<b>4.691</b>
	<b>0.67</b>	<b>2</b>	<b>34.095</b>	<b>4.722</b>	<b>3.383</b>
	<b>0.74</b>	<b>3</b>	<b>39.358</b>	<b>1.267</b>	<b>4.923</b>
	<b>0.80</b>	<b>4</b>	<b>32.235</b>	<b>-0.289</b>	<b>1.070</b>
	<b>0.96</b>	<b>5</b>	<b>35.764</b>	<b>3.311</b>	<b>3.338</b>
	<b>1.00</b>	<b>6</b>	<b>32.883</b>	<b>3.417</b>	<b>2.361</b>
	<b>1.16</b>	<b>7</b>	<b>19.559</b>	<b>2.867</b>	<b>1.754</b>
	<b>2.00</b>	<b>8</b>	<b>38.046</b>	<b>1.396</b>	<b>1.519</b>
	<b>2.52</b>	<b>9</b>	<b>38.021</b>	<b>-0.087</b>	<b>0.779</b>
<b>UP A5</b>	<b>0.66</b>	<b>1</b>	<b>20.360</b>	<b>0.702</b>	<b>-0.904</b>
	<b>0.87</b>	<b>2</b>	<b>41.569</b>	<b>8.280</b>	<b>0.923</b>
	<b>0.92</b>	<b>3</b>	<b>40.725</b>	<b>8.771</b>	<b>-0.020</b>
	<b>1.34</b>	<b>4</b>	<b>44.327</b>	<b>11.950</b>	<b>-0.492</b>
	<b>1.46</b>	<b>5</b>	<b>44.611</b>	<b>10.781</b>	<b>-1.420</b>
	<b>2.85</b>	<b>6</b>	<b>47.850</b>	<b>21.223</b>	<b>-1.891</b>
	<b>2.94</b>	<b>7</b>	<b>44.971</b>	<b>15.211</b>	<b>-0.378</b>
<b>DL A6</b>	<b>0.49</b>	<b>1</b>	<b>31.821</b>	<b>-5.695</b>	<b>0.215</b>
	<b>0.55</b>	<b>2</b>	<b>38.284</b>	<b>1.107</b>	<b>1.641</b>
	<b>0.64</b>	<b>3</b>	<b>38.769</b>	<b>-2.222</b>	<b>0.173</b>
	<b>0.68</b>	<b>4</b>	<b>37.664</b>	<b>0.801</b>	<b>0.103</b>
	<b>0.73</b>	<b>5</b>	<b>31.354</b>	<b>1.768</b>	<b>-0.067</b>
	<b>0.84</b>	<b>6</b>	<b>39.534</b>	<b>4.264</b>	<b>1.377</b>
	<b>0.97</b>	<b>7</b>	<b>41.610</b>	<b>-4.011</b>	<b>-0.527</b>
	<b>1.00</b>	<b>8</b>	<b>44.474</b>	<b>1.521</b>	<b>0.488</b>
	<b>1.99</b>	<b>9</b>	<b>37.185</b>	<b>0.001</b>	<b>0.789</b>
	<b>2.21</b>	<b>10</b>	<b>35.864</b>	<b>-0.705</b>	<b>0.481</b>
	<b>2.86</b>	<b>11</b>	<b>40.914</b>	<b>0.182</b>	<b>0.039</b>
<b>UP A6</b>	<b>0.93</b>	<b>1</b>	<b>51.822</b>	<b>16.966</b>	<b>-4.369</b>
	<b>1.17</b>	<b>2</b>	<b>45.272</b>	<b>13.677</b>	<b>-4.796</b>
	<b>1.27</b>	<b>3</b>	<b>45.960</b>	<b>14.642</b>	<b>-1.703</b>
	<b>2.19</b>	<b>4</b>	<b>49.415</b>	<b>12.783</b>	<b>-3.744</b>
	<b>2.26</b>	<b>5</b>	<b>47.212</b>	<b>13.180</b>	<b>-2.460</b>
<b>DL A7</b>	<b>0.44</b>	<b>1</b>	<b>34.549</b>	<b>2.938</b>	<b>0.569</b>
	<b>0.50</b>	<b>2</b>	<b>38.942</b>	<b>2.062</b>	<b>0.493</b>
	<b>0.54</b>	<b>3</b>	<b>46.592</b>	<b>3.306</b>	<b>0.814</b>
	<b>0.68</b>	<b>4</b>	<b>39.215</b>	<b>5.125</b>	<b>0.453</b>



	0.71	6	31.963	5.596	1.114
	0.84	7	30.308	6.219	2.537
	0.94	8	28.963	3.992	2.789
	1.00	9	22.347	3.222	1.498
	1.56	10	36.776	2.900	0.475
	2.72	11	31.717	-0.114	0.169
UP A7	0.65	1	37.062	3.874	1.905
	0.78	2	15.247	-3.701	0.828
	1.05	3	39.224	16.523	2.608
	1.13	4	37.711	6.207	1.150
	1.26	5	37.456	9.785	0.344
	1.81	6	41.674	5.133	2.998
SL A11	0.34	1	4.575	34.627	-0.920
(outer)	0.68	2	4.650	34.491	0.199
	0.91	3	5.299	35.551	0.180
	1.50	4	-0.150	34.716	-3.283
	2.89	5	0.210	35.364	-3.963
	3.54	6	0.399	37.840	-4.813
A12	0.79	1	-1.041	-50.402	-4.865
(inner)	1.86	2	0.057	-51.885	-0.074
	3.01	3	-0.152	-54.177	-2.844
	3.17	4	0.440	-54.082	-0.674
	3.21	5	0.830	-52.878	0.938

## **2.6 Velocity contour**

To get a better idea on the velocity distribution, velocity contour is drawn using the data found from the experiment conducted. For this purpose, 3DField is used. 3DField constructs 2D/3D maps of contours (isolines) on the base of numerical data.

Following are the figures showing velocity contour for different depth of flow

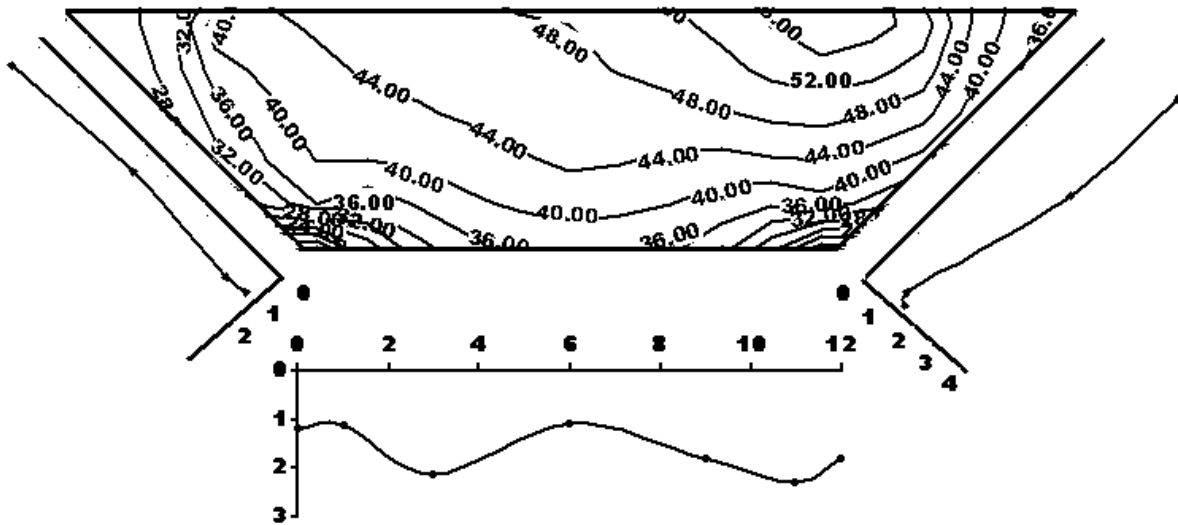


Fig. 1 Velocity Distribution for 6 cm depth of water

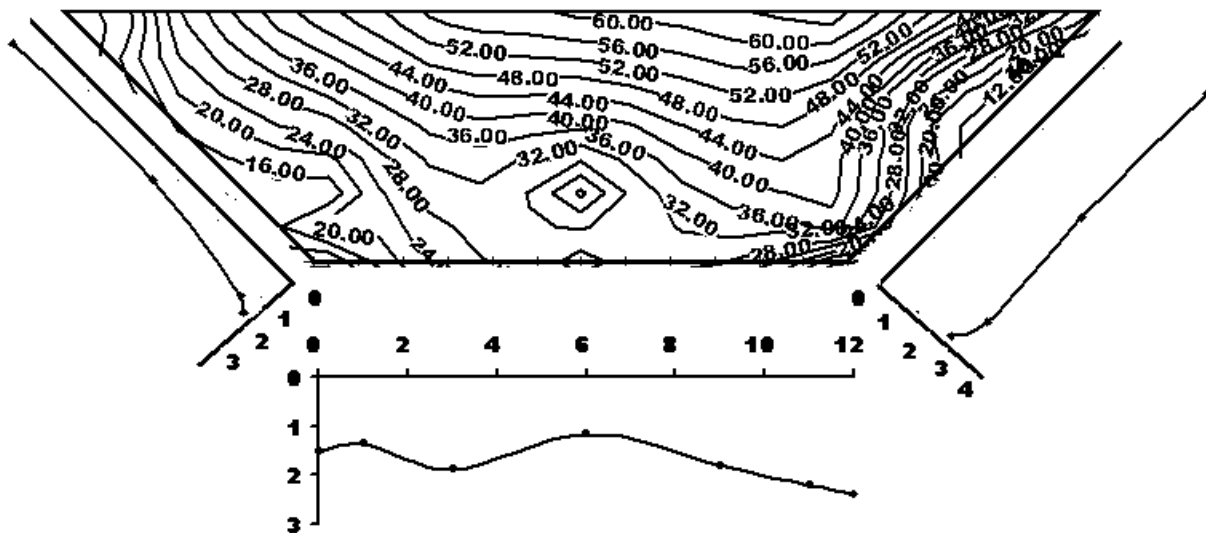


Fig. 2 Velocity Distribution for 6.4 cm depth of water

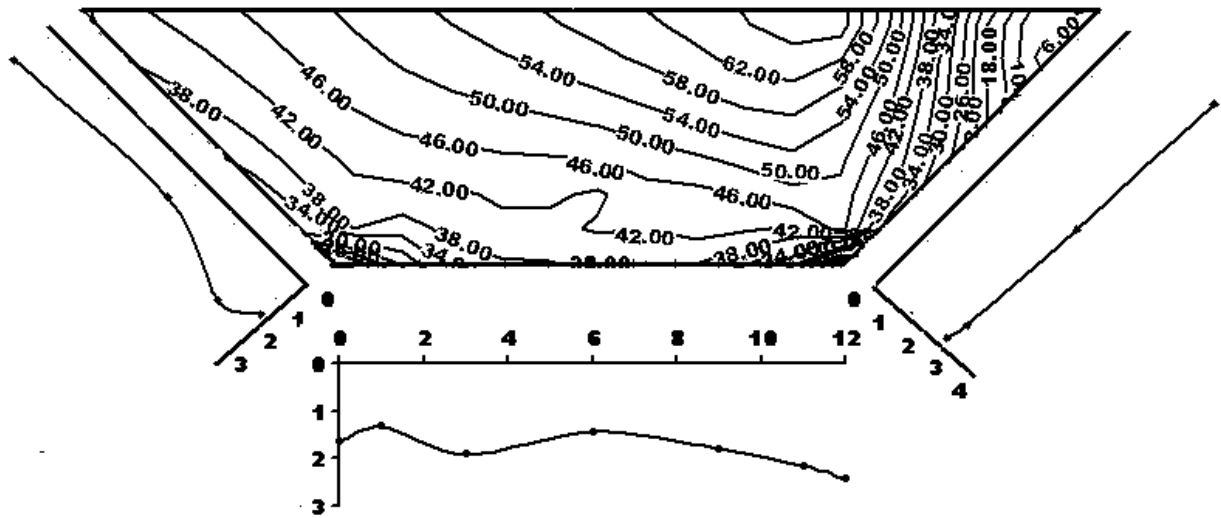


Fig. 3 Velocity Distribution for 7.2 cm depth of water

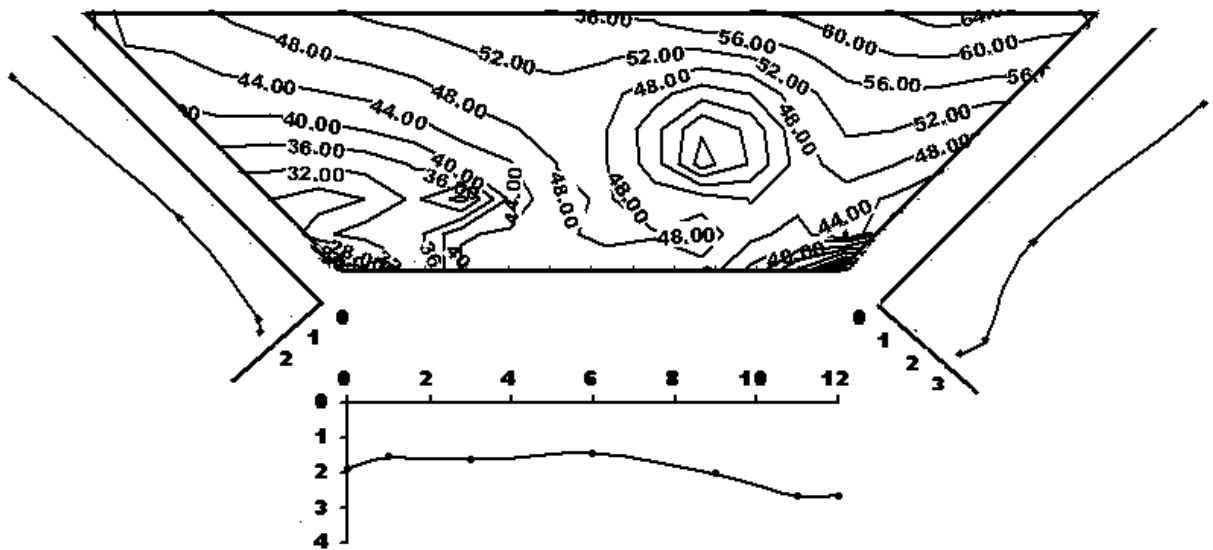


Fig. 4 Velocity Distribution for 7.9 cm depth of water

## 2.7 THEORETICAL ANALYSIS

What happens at a boundary?

What type of differencing is possible when we have only one direction to go, namely, the direction away from the boundary? For example, consider Fig. 1, which illustrates a portion of a boundary to a flow field, with the  $y$  axis perpendicular to the boundary. Let grid point 1 be on the boundary, with points 2, 3, 4 and 5 a distance  $\Delta y$ ,  $2\Delta y$ ,  $3\Delta y$  and  $4\Delta y$  above the boundary, respectively. We wish to construct a finite-difference approximation for  $(\partial u / \partial y)$  at the boundary. It is easy to construct a forward difference as

$$\left( \frac{\partial u}{\partial y} \right)_1 = \frac{u_2 - u_1}{\Delta y} + O(\Delta y) \quad (1)$$

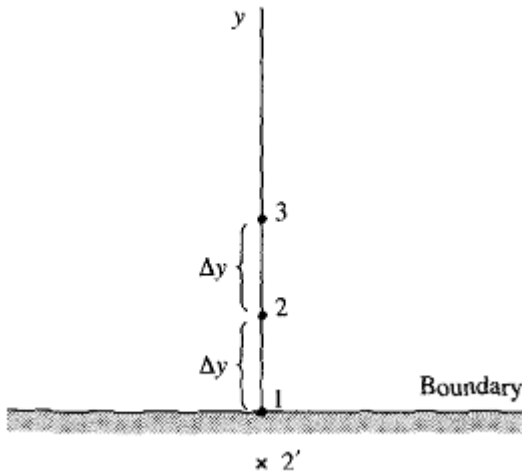


Fig 1. Grid Points at a boundary

which is of first-order accuracy. However, here we try to obtain a result which is of fourth-order accuracy. Our central difference in Eq. (4.11) fails us because it requires another point beneath the boundary, such as illustrated as point 2' in Fig. 1. Point 2' is outside the domain of computation, and we generally have no information about  $u$  at this point. In the early days of CFD, many solutions attempted to sidestep this problem by assuming that  $u_{2'} = u_2$ . This is called the reflection boundary condition. In most cases it does not make physical sense and is just as inaccurate, if not more so, than the forward difference given by Eq. (1). So how do we find a second-order-accurate finite-difference at the boundary? The answer is straightforward, as we will describe here. Moreover, we will seize this occasion to illustrate an alternative approach to the construction of finite-difference quotients--alternative to the Taylor's series analyses presented earlier. We will use a polynomial approach, as follows. Assume at the boundary shown in Fig. 1 that  $u$  can be expressed by the polynomial

$$u = a + by + cy^2 + dy^3 + ey^4 \quad (2)$$

Applied successively to the grid points in Fig. 1, Eq. (2) yields at grid point 1 where  $y = 0$ ,

$$u_1 = a \quad (3)$$

and at grid point 2 where  $y = \Delta y$ ,

$$u_2 = a + b(\Delta y) + c(\Delta y)^2 + d(\Delta y)^3 + e(\Delta y)^4 \quad (4)$$

and at grid point 3 where  $y = 2\Delta y$ ,

$$u_3 = a + b(2\Delta y) + c(2\Delta y)^2 + d(2\Delta y)^3 + e(2\Delta y)^4 \quad (5)$$

and at grid point 4 where  $y = 3\Delta y$ ,

$$u_4 = a + b(3\Delta y) + c(3\Delta y)^2 + d(3\Delta y)^3 + e(3\Delta y)^4 \quad (6)$$

and at grid point 5 where  $y = 4\Delta y$ ,

$$u_5 = a + b(4\Delta y) + c(4\Delta y)^2 + d(4\Delta y)^3 + e(4\Delta y)^4 \quad (7)$$

Solving Eqs. (3) to (7) for  $b$ , we obtain

$$b = \frac{-220u_1 - 84u_2 + 42u_3 + 44u_4 + 9u_5}{12\Delta y} \quad (8)$$

Returning to Eq. (2), and differentiating with respect to  $y$ ,

$$\frac{\partial u}{\partial y} = b + 2cy + 3dy^2 + 4ey^3 \quad (9)$$

Equation (9), evaluated at the boundary where  $y = 0$ , yields

$$\left( \frac{\partial u}{\partial y} \right)_1 = b \quad (10)$$

Combining Eqs. (8) and (10), we obtain

$$\left( \frac{\partial u}{\partial y} \right)_1 = \frac{-220u_1 - 84u_2 + 42u_3 + 44u_4 + 9u_5}{12\Delta y} \quad (11)$$

Equation (11) is a one-sided finite-difference expression for the derivative at the boundary called one-sided because it uses information only on one side of the grid point at the boundary, namely, information only above grid point 1 in Fig. 1. Also, Eq. (11) was derived using a polynomial expression, namely, Eq. (2), rather than a Taylor series representation. This illustrates an alternative approach to the formulation of finite-difference quotients. It remains to show the order of accuracy of Eq. (11). Here, we have to appeal to a Taylor series again. Consider a Taylor series expansion about the point 1.

$$u(y) = u + \left( \frac{u}{y} \right)_1 y + \left( \frac{\partial^2 u}{\partial y^2} \right) \frac{y^2}{2} + \left( \frac{\partial^3 u}{\partial y^3} \right) \frac{y^3}{6} + \dots \quad (12)$$

Compare Eqs. (12) and (2). Our assumed polynomial expression in Eq. (2) is the same as using the first three terms in the Taylor series. Hence, Eq. (4.20) is of  $O(\Delta y)^5$ . Now examine the numerator of Eq. (11); here  $u_1, u_2, u_3, u_4$  and  $u_5$  can all be expressed in terms of the polynomial given by Eq. (2). Since Eq. (2) is of  $O(\Delta y)^5$ , then the numerator of Eq. (11) is also of  $O(\Delta y)^5$ . However, in forming the derivative in Eq. (11), we divided by  $\Delta y$ , which then makes Eq. (11) of  $O(\Delta y)^4$ . Thus, we can write from Eq. (11)

$$\left(\frac{\partial u}{\partial y}\right)_1 = \frac{-220u_1 - 84u_2 + 42u_3 + 44u_4 + 9u_5}{12\Delta y} + O(\Delta y)^4 \quad (13)$$

This is our desired fourth-order-accurate difference quotient at the boundary. Both Eqs. (1) and (13) are called one-sided differences, because they express a derivative at a point in terms of dependent variables on only one side of that point. Moreover, these equations are general; i.e., they are not in any way limited to application just at a boundary; they can be applied at internal grid points as well. It just so happens that we have taken advantage of our discussion of finite-difference quotients at a boundary to derive such one-sided differences. Of course, as we have seen here, one-sided differences are essentially mandatory for a representation of a derivative at a boundary, but such one-sided differences simply offer another option when applied internally within the domain of the overall calculations. Furthermore, Eq. (13) displays a one-sided finite difference of fourth-order accuracy; many other one-sided difference formulas for a derivative at a point can be derived with higher orders of accuracy using additional grid points to one side of that point. In some CFD applications, it is not unusual to see four- and five-point one-sided differences applied at a boundary. This is especially true for viscous flow calculations. In such calculations, the shear stress and heat transfer at the wall, due to a flow over that wall, are of particular importance. The shear stress at the wall is given by,

$$\tau_w = \mu \left( \frac{\partial u}{\partial y} \right)_w \quad (14)$$

and the heat transfer at the wall is given by,

$$q_w = k \left( \frac{\partial T}{\partial y} \right)_w \quad (15)$$

In finite-difference solutions of a viscous flow (solutions of the Navier-Stokes equations, parabolized Navier-Stokes equations, the boundary-layer equations, etc.), the flow-field values of  $u$  and  $T$  are calculated at all the grid points, internal as well as boundary points. Then, after these flow-field values are obtained (by whatever algorithm is chosen), the shear stress and heat transfer are calculated after the fact from Eqs. (14) and (15). Clearly, the more accurate the one-sided finite difference used to represent  $(\partial u / \partial y)_w$  and  $(\partial T / \partial y)_w$  in Eqs. (14) and (15), respectively, the more accurate will be the calculated results for  $\tau_w$  and  $q_w$ .

### **3.BOUNDARY SHEAR STRESS DISTRIBUTION**

About seven decades ago, Leighly (1932) proposed the idea of using conformal mapping to study the boundary shear stress distribution in open-channel flows. He pointed out that, in the absence of secondary currents, the boundary shear stress acting on the bed must be balanced by the downstream component of the weight of water contained within the bounding orthogonal. This idea has not rendered any conclusive results (Graf, 1971, p.107), though Lundgren and Jonsson (1964) extended the logarithmic law to a parabolic cross-sectional open-channel and proposed a method to determine the shear stress. Chiu and Chiou (1986) extended the logarithmic law to rectangular cross-sections and provided an analytical method to compute the boundary shear stress. As pointed out by Nezu and Nakagawa (1993, p.91), the results calculated by Chiu and Chiou revealed large errors. Keulegan (1938) and Johnson (1942) contributed to the early development of this subject, and Einstein's (1942) hydraulic radius separation method (Chien and Wan 1983, p.195) is still widely used in laboratory studies and engineering practice. Einstein divided a cross-sectional area into two areas  $A_b$  and  $A_w$ . He assumed that the down-stream component of the fluid weight in area  $A_b$  is balanced by the resistance of the bed. Likewise, the downstream component of the fluid weight in area  $A_w$  is balanced by the resistance of the two side-walls. There is no friction at the interface between the two areas  $A_b$  and  $A_w$ . In terms of energy, the potential energy provided by area  $A_b$  is dissipated by the channels bed, and the potential energy provided by area  $A_w$  is dissipated by the two side-walls. Following this idea, Yang and Lim (1997, 1999) recently proposed an analytical method to determine the delimitations between the two areas in Fig. 1. However, their method is inconvenient for applications because of its implicit and segmental form (Guo 1999). Since 1960s, several experimental studies have been reported by Cruiff (1965), Ghosh and Roy (1970), Kartha and Leutheusser (1970), Myers (1978), Knight and Macdonald (1979), Knight (1981), Noutsopoulos and Hadjipanous (1982), Knight et al. (1984), Hu (1985), and others. Knight and his associates collected a great deal of experimental data about the effect of the side-walls at different width-depth ratios. With these data, they proposed several empirical relations which are very helpful in the studies of open-channel flow and sediment transport.

The wall shear stress distribution in a planar and axially symmetric flow is uniform along the wetted perimeter and shear stress can be calculated from force balance. However, for rectangular channels with a finite aspect ratio after a certain  $W/h$  ratio ( $W/h < 10$  in narrow channels), flow in the channel becomes three-dimensional and wall shear stress is not uniformly distributed due to the free surface and existence of secondary flows. Therefore, the calculation of the distribution of wall shear stress in a rectangular open channel is complex

Different researches have considered the shear distribution problem by obtaining local shear stress as a fraction of the total shear stress and as a function of the aspect ratio  $B/y$ , where  $B$  is the channel width and  $y$  is the depth. In this paper, it is intended to verify that experimental data related to shear stress show similar results for if they keep



geometric similitude. It is also intended to find the influence of the aspect ratio on shear stresses at the boundaries.

For steady uniform flow in an open channel, gravity forces causing the flow must be equal to boundary shear forces. The channel depth is approximately equal to the hydraulic radius  $R_h$  for a very wide-open channel.  $R_h$  is equal to the ratio of the cross-section area  $A$  to the wetted perimeter  $P$ . Therefore, the shear stress at the channel bed is expressed as

$$\tau_o = \rho g R_h S$$

where  $\tau_o$  shear stress along the bed boundary,  $\rho$  flow density,  $g$  acceleration due to the gravity,  $S = H_f / L$  represents the slope of the energy grade line,  $H_f$  is energy loss due to friction, and  $L$  is the length of the channel where boundary shear stress occurs.

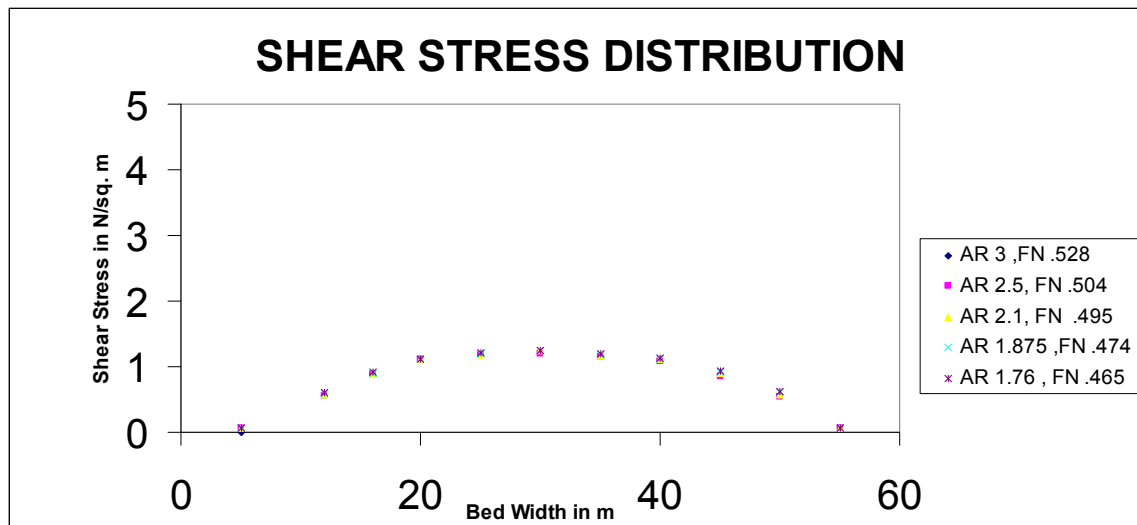


Fig. Shear Stress Distribution in open channel

## **4.Numerical evaluation of boundary shear distribution in meandering channels**

Information on the nature of boundary shear stress distribution in simple and meandering open channel are required to solve a variety of river hydraulics and engineering problems so as to give a basic understanding of the resistance relationship, calculation of energy losses, to understand the mechanism of sediment transport, to design stable channels, revetments etc. Distribution of boundary shear stress depends mainly on the shape of the channel cross section and the structure of the secondary flow cells. Most of the hydraulic formulae assume that the boundary shear stress distribution is uniform over the entire wetted perimeter of an open channel. However in a meandering channel, the complex flow mechanism causes significant variation in the distribution of shear that is, increasing the shear at the inner region and decreasing near the outer part of the channel. Therefore, there is a need to evaluate the boundary shear stress distribution at various locations of the wetted perimeter. The velocity, resistance and boundary shear stress distribution in meandering channels section have also been investigated by many authors e.g. [1], [2], [3], [4], [5], Study of literature shows that the investigators have studied the boundary shear distribution mostly for shallow channels having sinuosity. Boundary shear distribution for deep and highly meandering channels are not available.

The work presented in this paper is based on series of highly meandering channels having distinctly different sinuosity and geometry. Experiments are carried out to examine the effect of secondary currents, channel sinuosity, and cross section geometry on the value of boundary shear. First the 3-dimensional velocities at a number of pre defined grid points across the channel section are measured using 16-Mhz Micro ADV (Acoustic Doppler Velocity-meter). Using these velocity data close to the surface, the boundary shear at various points on the channel boundaries are evaluated from semi log plot of velocity distribution as well as by using numerical finite difference solution. Error adjustments to the shear value by the two methods are done by comparing the corresponding shear value obtained from the energy gradient approach. The results so obtained between the two methods are consistently within  $\pm 3$ . Based on the present experimental and numerical results, this paper predicts the distribution of boundary shear in a highly meandering channel thus showing the interrelationship between the boundary shear, sinuosity and geometrical parameters. The models are also validated using the well published data of other investigators.

### **PREVIOUS WORK**

The velocity, resistance and boundary shear stress distribution in meandering channels section have also been investigated by many authors e.g. [1], [2], [3], [4], [5], Study of literature shows that the investigators have studied the boundary shear distribution mostly for shallow channels

having sinuosity. Boundary shear distribution for deep and highly meandering channels are not available.

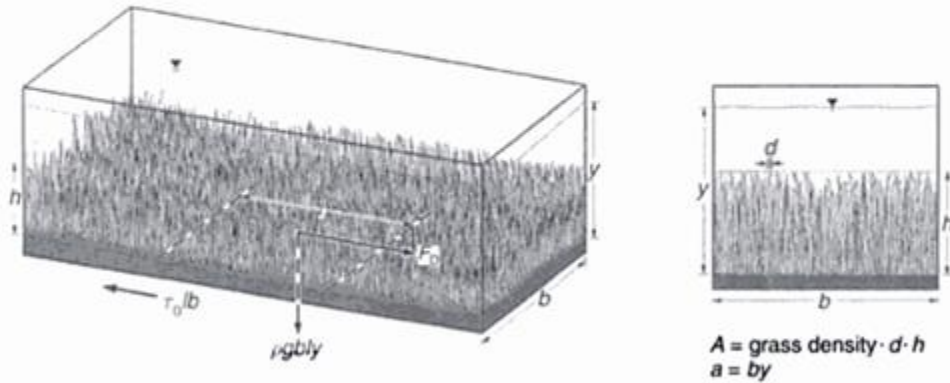


Figure 15.4 Definition of notation used by Wilson and Horritt (2002).

Using the general formula for fluid flowing past an immersed body, the drag force may be described by

$$F_D = \frac{1}{2} C_D \rho A U^2 \quad (15.5)$$

In which  $C_D$  = drag co-efficient of the vegetation;  $U$  = average longitudinal velocity;  $A$  = momentum-absorbing area of the vegetation; and  $\rho$  = density of water. The momentum absorbing area,  $A$ , and the ratio  $A/a$  (where  $a$  is the cross-sectional flow area) were phrases first coined by Fathi-Maghadam and Kouwen (1997). For sub-merged grass the projected area or momentum absorbing area is defined in Figure 15.4. The shear stress  $\tau$  and the drag force  $F_D$  can easily be converted to resistance co-efficients. From the definition of the Darcy-Weisbach friction factor,  $f$ ,

$$f = 8 \frac{\tau_0}{\rho U^2} \quad (15.6)$$

Equation (15.6) becomes:

$$f = 4 C_D \left( \frac{A}{b l} \right) \quad (15.7)$$

Or in terms of the Manning-Strickler friction co-efficient:

$$n = \frac{1}{2g} R^{1/3} C_D \left( \frac{A}{b l} \right) \quad (15.8)$$

## Results and discussion

For all grass heights and types, the hydraulic resistance significantly decreases with increasing flowing flow depth, tending towards an asymptotic constant which is reached at

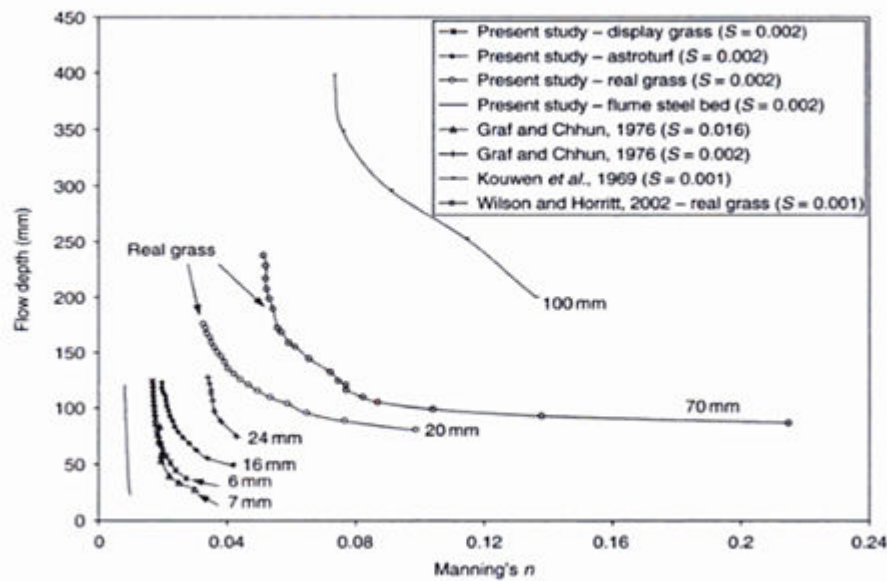


**Figure 15.5** Variation of Manning's  $n$  with flow depth for various grass linings. Undeflected grass height is annotated for each curve.

different levels of submergence depending on the grass properties (Figure 15.5). This can be explained by the fact that the exposure of the grass or the momentum-absorbing area is more pronounced as the depth increases. The ratio  $A/a$  decreases with increasing flow depth and therefore as the cross-sectional flow area increases Manning's  $n$  will decrease. Graf and Chhun (1976) and Kouwen et al. (1969) conducted similar experiments using artificial grass and arrays of flexible elements respectively, and they observed a similar relationship between  $n$  and flow depth (see Figure 15.5).

For the shorter grass height (7 mm) examined in the Graf and Chhun study the asymptotic Manning's  $n$  value tends towards the same value as observed in this study ( $n = 0.017$ – $0.019$ ). However, as the flow depth decreases, the Manning's  $n$  curves corresponding to heights 6 and 7 mm deviate. This is probably related to the thickness of the interaction zone directly above the grass canopy which is dependent on grass height and grass properties. For taller grass heights ( $h > 7$  mm) there is a significant increase in Manning's  $n$  with increasing flow depth and for the real grasses the constant Manning's  $n$  value is dependant on the grass height whereby for undeflected grass heights 20 mm and 70 mm the value varies from 0.033 to 0.052, respectively. The actual value of  $n$  for the taller grass is 40% greater than that usually given for short grassy floodplains in well-established texts (Chow, 1959), but relatively lower than values predicted using the USDA handbook method and the method of Green and Garton (1983). These methods over-predict the Manning Strickler co-efficient by 140 and 167% respectively (Figure 15.6). This value also

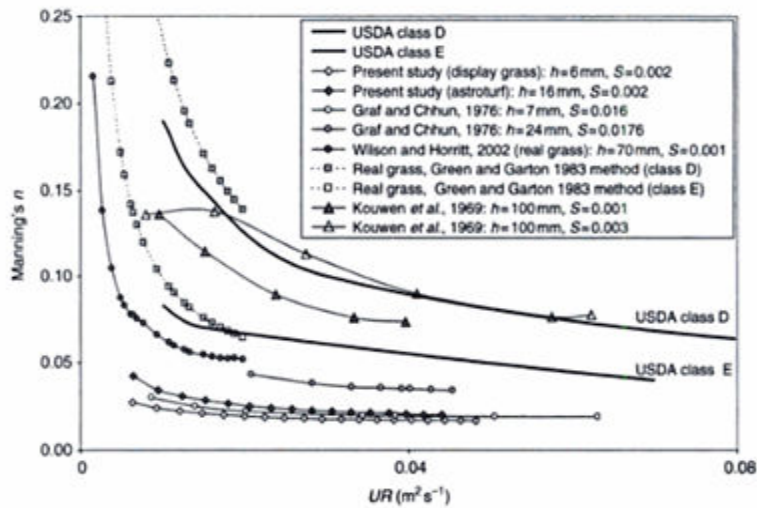


**Figure 15.6** Relationship of Manning's  $n$  roughness coefficient as a function of the product of mean area velocity and hydraulic radius.

corresponds well with the values found from calibration studies of reach length (10-60km) 2D hydraulic models of compound channel flow (Horrit and Bates, 2001). For all types examined, the vertical profile of time-averaged stream wise velocity is similar (Figure 15.7). Profiles for all canopies show significant variation in the mean velocity and indicate the generation of a horizontal shear layer. Within the canopy the mean flow is much retarded and immediately above the grass layer there is a significant increase in mean velocity with increasing flow depth. The profiles corresponding to the display grass and Astroturf tend towards convergence.

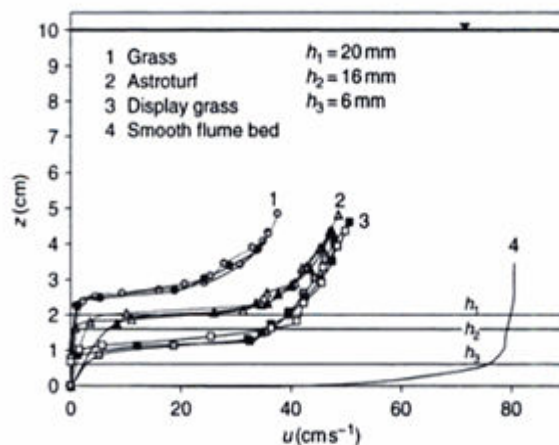


**Figure 15.7** Time-averaged streamwise velocities for different grass linings.

## **5.RESULTS**

For Depth=6cm

Point	u1	u2	u3	dely	Derivative	Boundary Shear
A1	16	20	24	0.09	577.7777778	0.577777778
A2	36	40	44	0.09	1244.444444	1.244444444
A3	36	40	44	0.09	1244.444444	1.244444444
A4	20	24	28	0.09	711.1111111	0.711111111
SL1	32	36	40	0.09	1111.111111	1.111111111
SL2	28	32	36	0.09	977.7777778	0.977777778
SR1	36	40	44	0.09	1244.444444	1.244444444

For Depth=6.4cm

Point	u1	u2	u3	dely	Derivative	Boundary Shear
A1	20	24	28	0.09	711.1111111	0.711111111
A2	32	36	40	0.09	1111.111111	1.111111111
A3	32	36	40	0.09	1111.111111	1.111111111
A4	24	28	32	0.09	844.4444444	0.844444444
SL1	16	20	24	0.09	577.7777778	0.577777778
SL2	16	20	24	0.09	577.7777778	0.577777778
SR1	24	28	32	0.09	844.4444444	0.844444444

For Depth = 7.2cm

Point	u1	u2	u3	dely	Derivative	Boundary Shear
A1	22	26	30	0.09	777.7777778	0.777777778
A2	38	42	46	0.09	1311.111111	1.311111111
A3	38	42	46	0.09	1311.111111	1.311111111
A4	22	26	30	0.09	777.7777778	0.777777778
SL1	34	38	42	0.09	1177.777778	1.177777778
SL2	38	42	46	0.09	1311.111111	1.311111111
SR1	34	38	42	0.09	1177.777778	1.177777778

For Depth = 7.9cm

Point	u1	u2	u3	dely	Derivative	Boundary Shear
A1	24	28	32	0.09	844.4444444	0.844444444
A2	44	48	52	0.09	1511.111111	1.511111111
A3	48	44	40	0.09	1555.555556	1.555555556
A4	16	20	24	0.09	577.7777778	0.577777778
SL1	28	32	36	0.09	977.7777778	0.977777778
SL2	40	44	48	0.09	1377.777778	1.377777778
SR1	44	48	52	0.09	1511.111111	1.511111111



## **6.VALIDATION OF RESULTS:**

The boundary shear stresses are calculated using two approaches. In the first approach the boundary shear stress is evaluated using polynomial processing method of CFD. Second approach is the Energy gradient method. This is a very traditional calculation in which for any trapezoidal channel under uniform flow conditions sum of boundary shear forces acting on the main channel wall and bed shall be equal to the resolved weight force along main channel .The observations are included in the table given below:-

Serial No:	Channel depth (in cm)	Average derivatives	Boundary shear stress by CFD(kg/m <sup>2</sup> )	Weighted perimeter	Gravity g(M <sup>2</sup> /S)	slope	Boundary shear stress (kg/cm <sup>2</sup> )	% of error
D=6.0(cm)	6.0	932.7	.9327	54	9.81	0.0054	.988	5.533
D=6.4(cm)	6.4	992.388	.992388	57.6	9.81	0.0054	1.0	7.12
D=7.2(cm)	7.2	1044.375	1.044375	64.8	9.81	0.0054	1.062	1.6
D=7.9(cm)	7.9	1266.625	1.266	71.1	9.81	0.0054	1.344	7.8

## **7.CONCLUSIONS**

In order to determine shear stresses at the bed and at the walls of smooth rectangular channels, experimental data available in the literature have been analysed both for smooth channels and for ducts. Functional relationships between shear stress at the walls and at the bed have been analysed as a function of mean shear stresses. Power expressions with correlation degrees higher than 0.90 have been obtained. Logarithmic experimental relationships for a wide data field are given in Eqs. 4, 5, 6 and 7 for the dimensionless shear stresses. Their correlation degrees are higher than 0.80 both for ducts and for open channel flow.

## **8.Reference:**

1. Bhattacharya, A. K. (1995). "Mathematical model of flow in meandering channel." PhD thesis, IIT, Kharagpur, India.
2. Ghosh, S.N., and Kar, S.K., (1975), "River Flood Plain Interaction and Distribution of Boundary Shear in a Meander Channel with Flood Plain", *Proceedings of the Institution of Civil Engineers, London, England*, Vol.59, Part 2, December, pp.805-811.
3. Greenhill, R.K. and Sellin, R.H.J., (1993), "Development of a Simple Method to Predict Discharge in Compound Meandering Channels", *Proc. of Instn. Civil Engrs Wat., Merit and Energy*, 101, paper 10012, March, pp. 37-44.
4. Knight, D.W., and Demetriou, J.D., (1983), "Flood Plain and Main Channel Flow Interaction". *Journal of Hyd. Engg., ASCE* Vol.109, No.8, pp-1073-1092.
5. Knight, D.W., and Shino, K. (1996). "River Channel and Floodplain Hydraulics. Floodplain Processes.", Edited by M.G.Anderson, Des E.Walling and Paul D.
6. Myers, W.R.C., (1987), "Velocity and Discharge in Compound Channels", *Jr. of Hydr. Engg., ASCE*, Vol.113, No.6, pp.753-766.
7. Myer, W.R.C., and Lyness, J.F., (1997), "Discharge Ratios in Smooth and Rough Compound Channels", *Jr. of Hydr. Eng., ASCE*, Vol., 123, No.3, pp.182-188.
8. Odgaard, A.J., (1986), "Meander Flow Model I : Development", *Jr. of Hyd.Engg., ASCE*, Vol 112, No.12, pp.1117-1135.
9. Odgaard, A.J., (1989), "River Meander Model-I :Development", *Journal of Hydr. Engineering, ASCE*, Vol., 115, No.11, pp.1433-1450.
10. Patra,K.C.,Kar,S.K.,(2000) Flow interaction of Meandering River with Flood plains *Journal of Hydr. Engineering, ASCE*, Vol., 126, No.8, pp.593-603.
11. Shiono, K., , Al-Romaih, J. S. and Knight D. W. "stage-discharge assessment in compound meandering channels" *journal of hydraulic engineering ASCE/April 2004/ 305*
12. Shiono K. & Knight, D.W., (1990), "Mathematical Models of Flow in two or Multistage Straight Channels", *Proc. Int. Conf. on River Flood Hyd.*, (Ed. W.R.White), J. Wiley & Sons, Wallingford, September, Paper G1, pp 229-238.

13. Shiono K., and Knight, D. W. (1989), “Two dimensional analytical solution of compound channel” *Proc., 3rd Int. Symp. on refined flow modeling and turbulence measurements*, Universal Academy Press, pp.591–599.
14. Shiono, K., and Knight, D. W. (1991). “Turbulent Open Channel Flows with Variable Depth Across the Channel.” *J. of Fluid Mech.*, Cambridge, U.K., 222, pp.617–646

## 9.Photo Gallery:























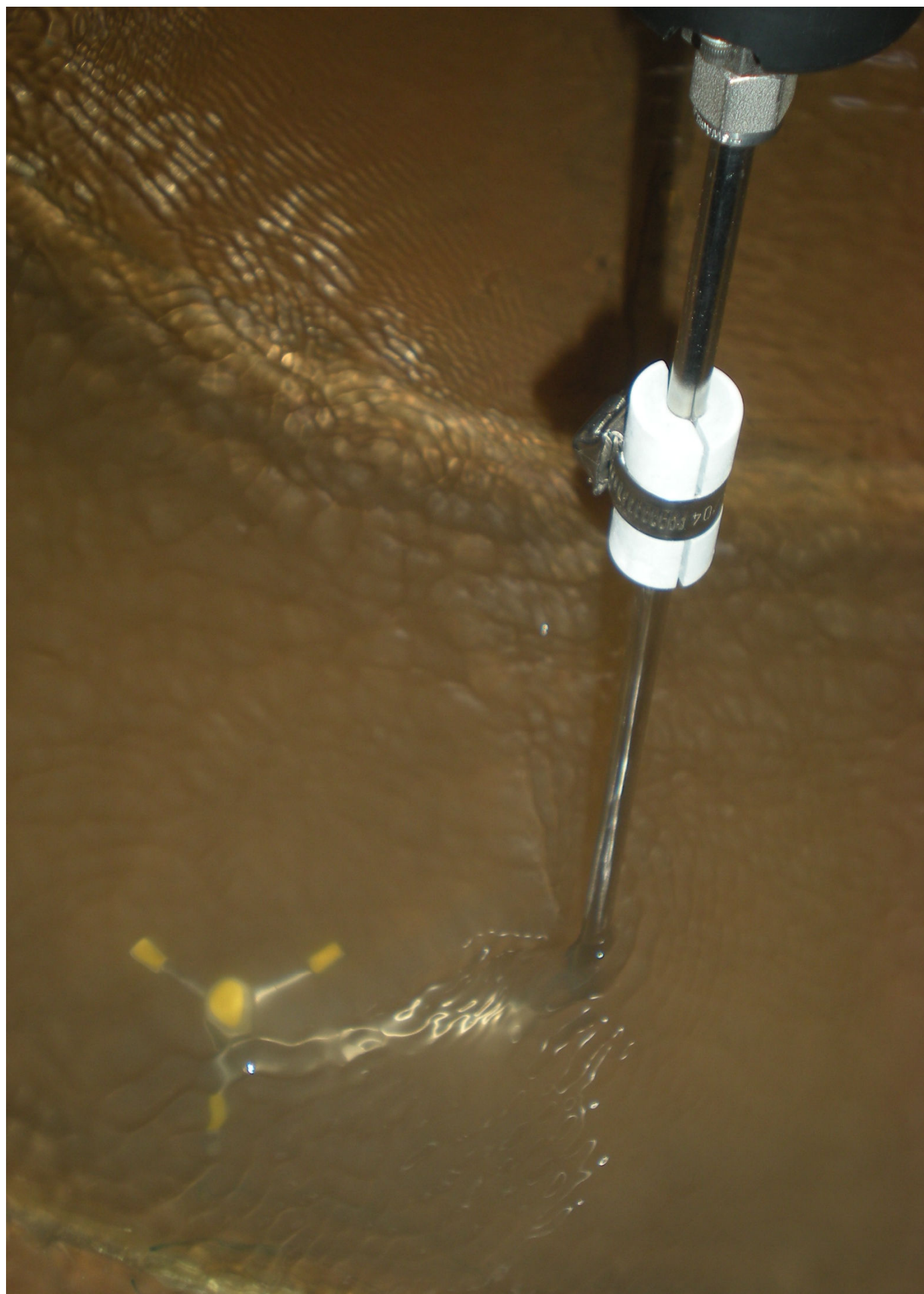




































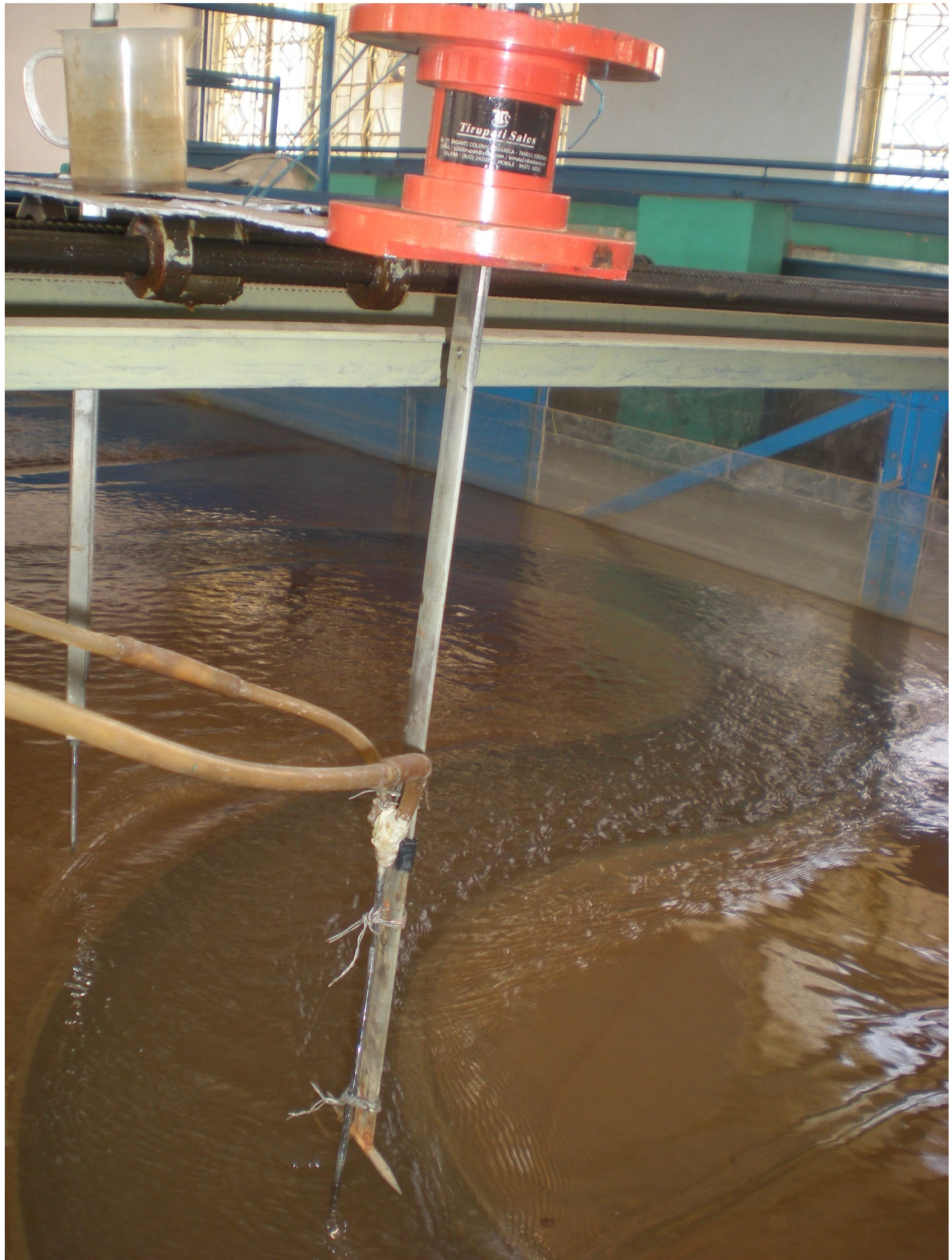
































MICRO-ACOUSTIC DOPPLER VELOCITY  
METER







